

# Appendix 1:

## Global Risk Analysis

---

1.1 Note on Methodology

1.2 Extraction of exposure and others parameters

ANNEX : Modelling Risk.....	1
1. Tropical Cyclones .....	4
1.1. Authors.....	4
1.2. Hazard .....	4
Modelling winds.....	4
Modelling storm surges .....	6

Sum of windspeed .....	9
From windspeed buffers to frequencies .....	9
Difficulties and limitations .....	9
Next steps.....	9
1.3. References.....	9
Articles and books .....	9
Internet references .....	10
Data sources .....	10
2. Floods .....	11
2.1. Authors.....	11
2.2. Hazard .....	11
Modelling flood .....	11
Observed flood events .....	12
Difficulties and limitations .....	14
2.3. References.....	15
Articles and books .....	15
2.4. Data sources.....	15
3. Drought .....	17
3.1. Authors.....	17
3.2. Hazard .....	17
Modelling droughts .....	17
Difficulties and limitations .....	21
Next steps.....	21
3.3. References.....	21
Articles and books .....	21
Internet references .....	22
3.4. Data sources.....	22
4. Landslides.....	23
4.1. Authors.....	23
4.2. Hazard .....	23
Modelling landslides .....	23
Difficulties and limitations .....	26
Next steps.....	26
4.3. References.....	27
Articles and books .....	27
4.4. Data Sources .....	27
5. Earthquakes.....	28
5.1. Authors.....	28
5.2. Hazard .....	28
Modelling Modified Mercalli Intensities (MMI) .....	30
From MMI to frequencies .....	31
Difficulties and limitations .....	31
Next steps.....	31

5.3.	References.....	31
5.4.	Data sources.....	31
6.	Tsunamis .....	32
6.1.	Authors.....	32
6.2.	Hazard .....	32
	Modelling tsunami .....	34
	Intensity .....	34
	Difficulties and limitations .....	35
	Next steps.....	35
6.3.	References.....	35
	Articles and books .....	35
	Internet references .....	35
6.4.	Data sources.....	36
7.	Biomass fires .....	37
7.1.	Authors.....	37
7.2.	Hazard .....	37
	Modelling Fires .....	37
7.3.	References.....	38
	Articles and books .....	38
7.4.	Data sources.....	38

## 1. Tropical Cyclones

### 1.1. Authors

*Cyclones winds hazard model (UNEP/GRID-Europe)*

Bruno Chatenoux

Pascal Peduzzi

based on previous work from Christian Herold, Frédéric Mouton, Ola Nordbeck and Pascal Peduzzi

*Cyclones storm surges hazard model (UNEP/GRID-Europe)*

Andrea De Bono

*Hazard methodology reviewed by:*

Jim DAVIDSON (Regional Director, Bureau of Meteorology, Queensland, Australia)

Woo-Jin LEE (Korean Meteorological Administration, Seoul, Republic of Korea)

Linda Anderson-Berry (Manager, Disaster Mitigation Policy and Emergency Management

Coordination, Weather and Ocean Services Policy Branch, Bureau of Meteorology, Melbourne, Australia)

*Focal points in WMO Secretariat:*

Koji Kuroiwa (Chief, Tropical Cyclone Programme, WMO)

Taoyong Peng (Tropical Cyclone Programme, WMO)

### 1.2. Hazard

Tropical cyclones are powerful hydro-meteorological hazards. On average, over 78 million people are affected globally by between 50 to 60 events each year. Tropical cyclones are unevenly spread around the globe (see Figure 1) as their development depends on specific climatic and oceanic conditions. A tropical cyclone has multiple impacts on the affected areas, including:

- Extremely powerful winds.
- Torrential rains leading to floods and/or landslides.
- High waves and damaging storm surge, leading to extensive coastal flooding.

The complexity of the multiple forms of impact triggered by tropical cyclones would call for integrated modelling of wind, rain, storm surge and landslides. However given the limited time available for the present study, priority was given to modelling the winds and storm surge.

#### *Modelling winds*

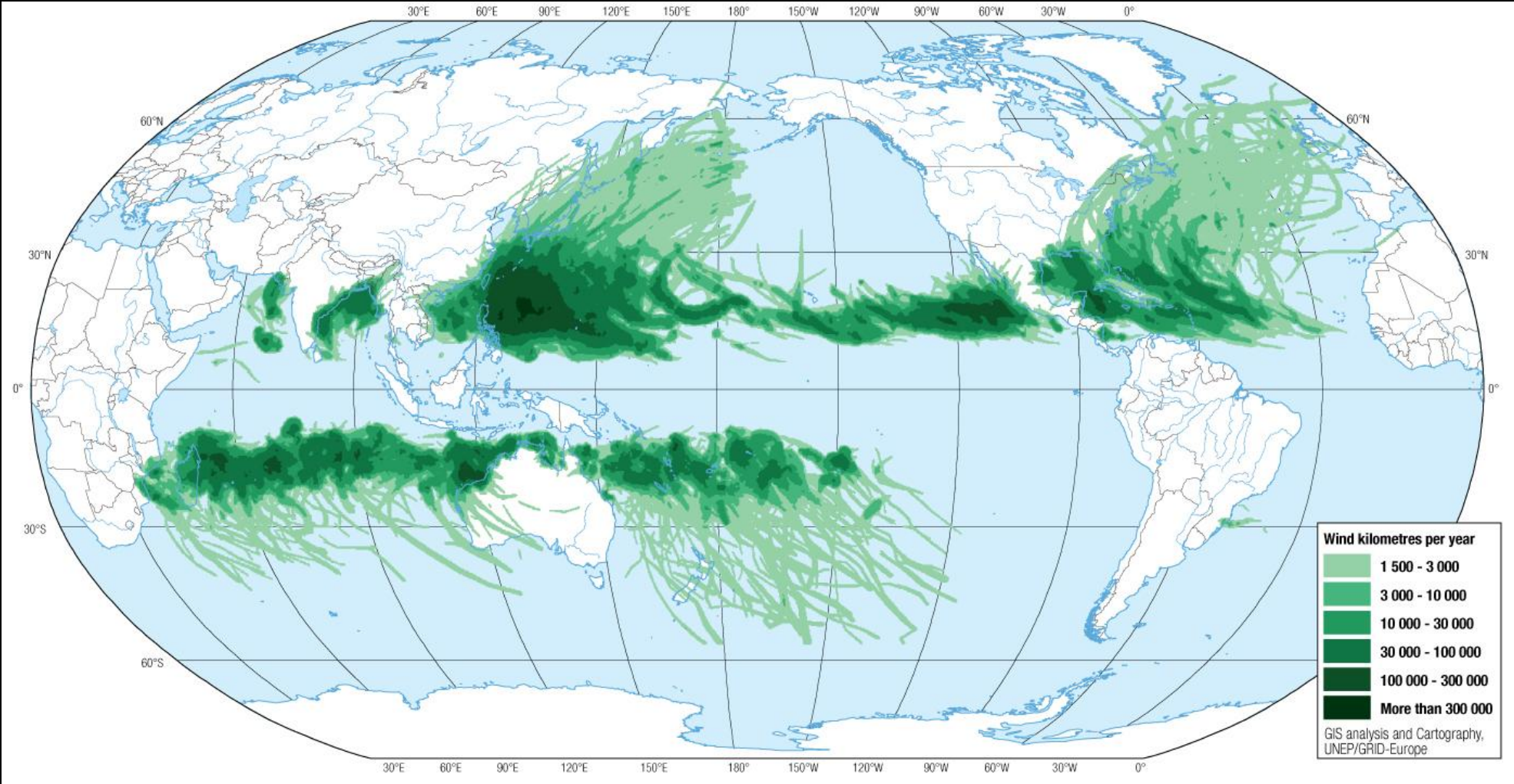
The proposed global model of tropical cyclones wind hazard is based on the observations of 2821 historical cyclone events through an estimation of the radial wind speed profile using a parametric model. The model is based on an initial equation from Holland (1980), which was further modified to take into consideration the movement of the cyclones through time. It is an update of the original data set (Herold et al. 2003)<sup>1</sup> developed by UNEP/GRID-Europe between 2001-2003 (see Nordbeck, Mouton and Peduzzi, 2005 for the detailed methodology). The dataset was made available by the United Nations Environment Programme (UNEP) under the name *PREVIEW Global Cyclones Asymmetric Wind speed profiles* (see Global Risk Data Platform) and other derived products (wind sum, frequency and physical exposure) were used (Peduzzi et al. 2002, Dao and Peduzzi 2004 to compute the Disaster Risk Index (DRI) published by United Nations Development Programme (UNDP 2004).

The previous model was covering 1980 – 2004 but had only 8 years in North Indian Ocean. This version was further improved by extending the time coverage from 1975 to 2007. It is spatially globally complete, except over South India Ocean where two years are missing (1975 and 1976). This is the reason why the study period of 30 years starts in 1977. Otherwise it is very complete, even the information on the 2004 Catarina cyclones that affected Brazil (south Atlantic) was also modelled (data courtesy of Anteon Corp./Roger Edson 2004, <http://cimss.ssec.wisc.edu/tropic/brazil/brazil.html>).

---

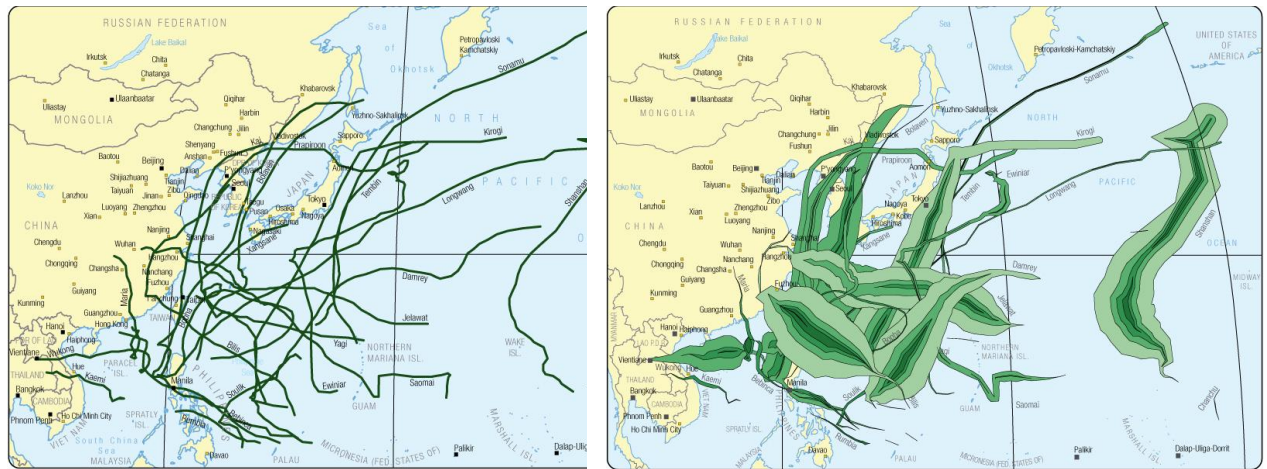
<sup>1</sup> [http://www.grid.unep.ch/activities/earlywarning/preview/data/trop\\_cycl/trop\\_cycl.php](http://www.grid.unep.ch/activities/earlywarning/preview/data/trop_cycl/trop_cycl.php)

Figure 1 Tropical cyclone intensities over the period 1977 – 2006 (sum of wind)



Practically the model transforms cyclone tracks (see Figure 2 on the left) into area affected according to the category of windspeed (see Figure 2 on the right). Each category corresponds to a given Saffir-Simpson intensity (see Table 1).

**Figure 2: From best tracks to Saffir-Simpson buffers**



**Table 1: Saffir-Simpson scale**

Category	Pressure (hPa)	Winds (km/h)	Surge (meters)
Tropical depression	---	---	---
Tropical storm	---	---	---
Category 1	More than 980	118 – 153	Less than 2
Category 2	965 – 980	154 – 177	2 – 3
Category 3	945 – 965	178 – 210	3 – 4
Category 4	920 – 945	211 – 249	4 – 5
Category 5	Less than 920	More than 259	5 – 10

Sources: Adapted from the U.S. National Oceanic and Atmospheric Administration (NOAA), National Hurricane Center (NHC)<sup>2</sup>

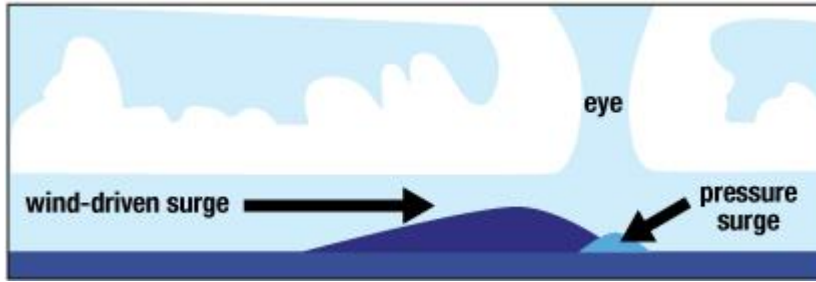
### Modelling storm surges

A storm surge is a high flood of water caused by wind and low pressure, most commonly associated with tropical cyclones. The strong winds blowing towards the shore help push water towards shore on the right side of the tropical cyclone's direction of motion. In addition, the central pressure of a tropical cyclone is so low that the relative lack of atmospheric weight above the eye and eye wall causes a bulge in the ocean surface level (Figure 3).

Storm surge is the main cause of most coastal flooding events. A storm surge is different from a tidal surge, which is a violent surge of water caused exclusively by the tidal shift in sea level. Typical storm surge heights vary with the hurricane's intensity, but they can range from less than one to more than 5 metres (Table 1). In the United States in 2005, the storm surge associated with Hurricane Katrina reached 9 metres in some locations.

<sup>2</sup> [www.nhc.noaa.gov/abouttssh.shtml](http://www.nhc.noaa.gov/abouttssh.shtml)

**Figure 3 Schema of storm surges**



Source: Robert Simmon, NASA GSFC, 2007

The data used to map surge hazard are based on a very detailed elevation model at 90 m of resolution (SRTM). The first 10 km inland from the coastal line were retained for the analysis. In the Saffir–Simpson scale, each intensity category also specifies the range of amplitude for storm surge waves (Table 1). The intersection of cyclone tracks on our coastal buffer designates regions that can potentially be impacted by a given cyclone intensity: for example, all the coastal zones having elevation  $\leq$  to 2 meters can be potentially impacted by a surge associated with a Saffir-Simpson category 1 storm.

Tide effects have not been taken into account, even if it could be done for individual events (Figure 4). For a global modelling over more than 30 years, this was quickly disregarded given the time at disposal. The other improvements that should be introduced are to incorporate coastal protection from natural features, including vegetation and coastal topography.

This simplified model is flooding all areas below the height of the storm wave, the case where a natural or built dikes exist protecting a lower lying ground further inland is not considered. This can lead to some exaggeration, but for a global model, using a 90 meters resolution is already very accurate and fits quite well with observed flooded areas as detected by satellite sensors (see Figure 4).

**Figure 4 Nargis 2008: simulated storm surge, including tide effect and observed flooded zones**

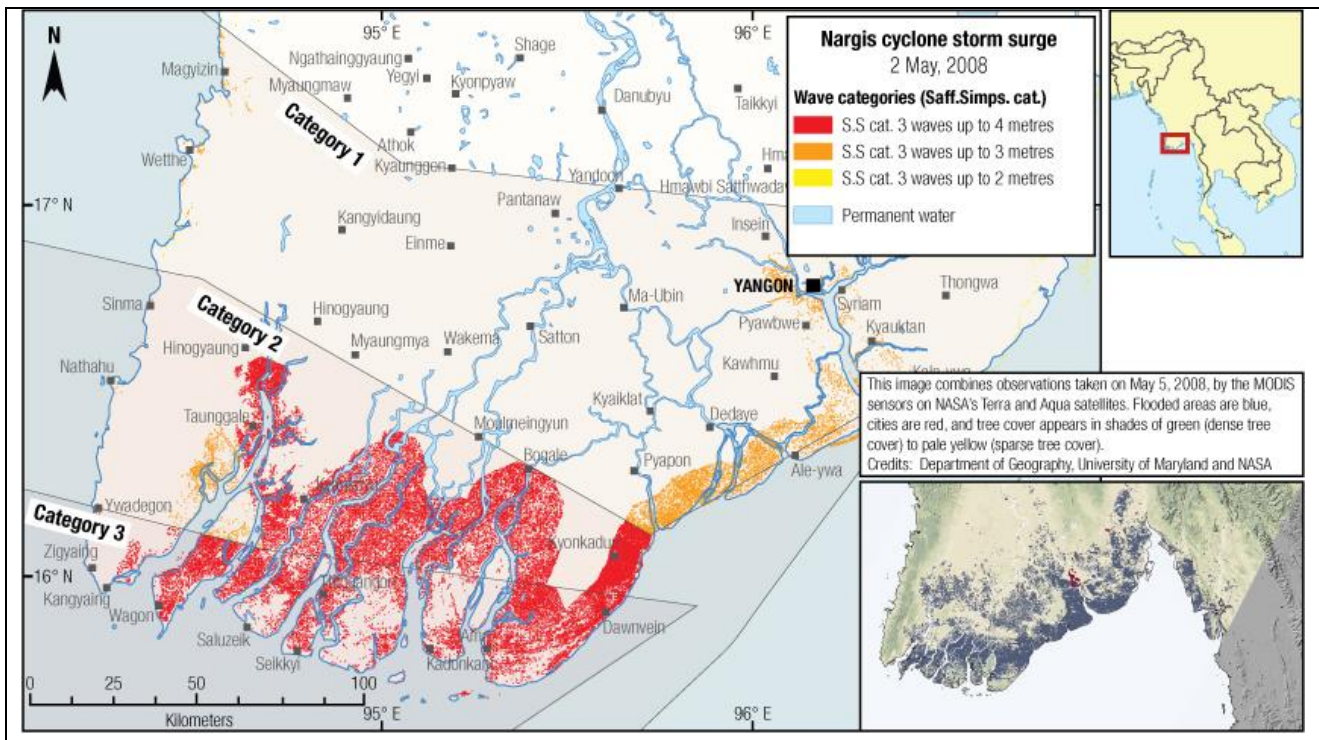
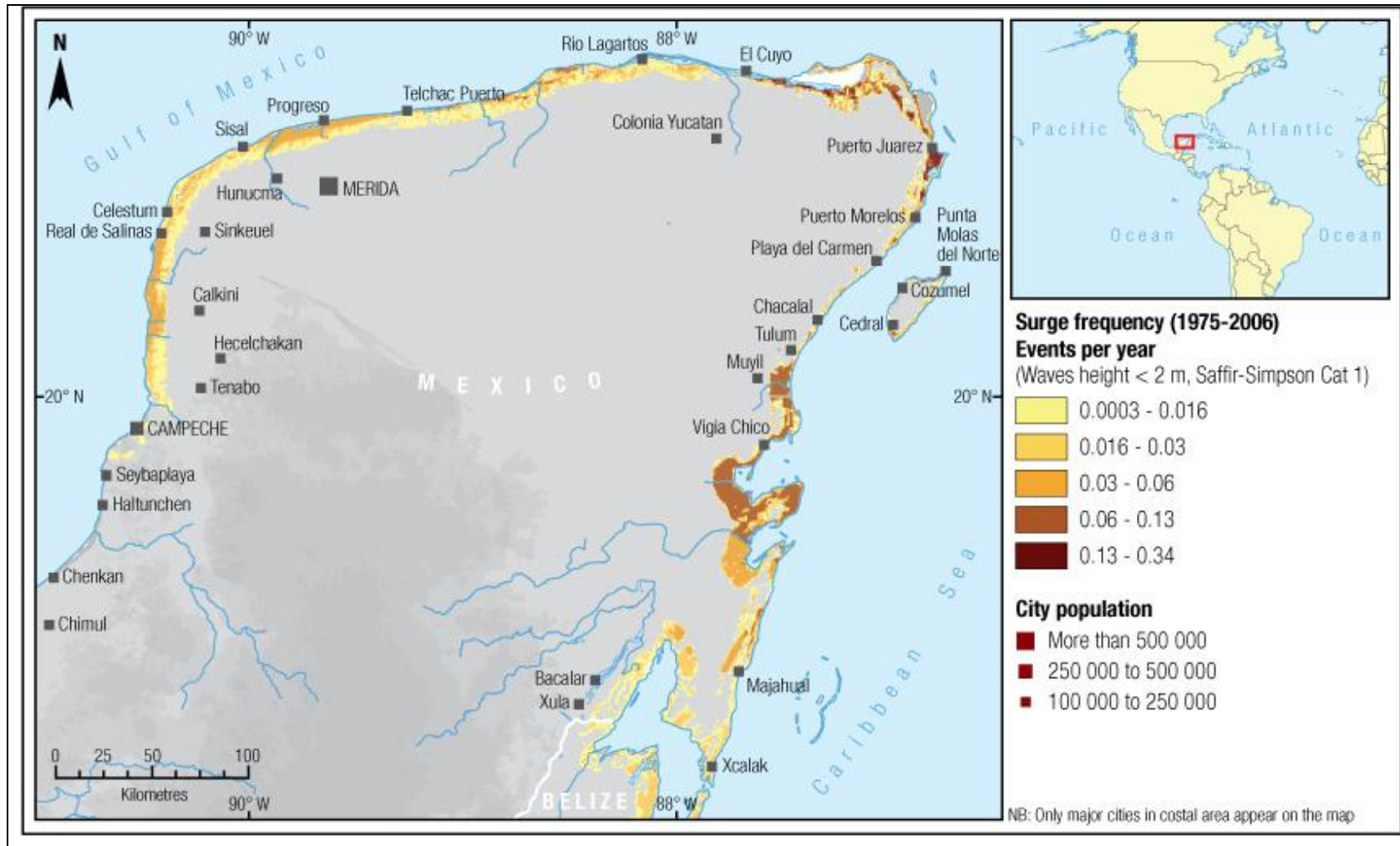


Figure 5 Surge frequency in the Caribbean region: intensities 1 from Saffir-Simpson scale are shown



### *Sum of windspeed*

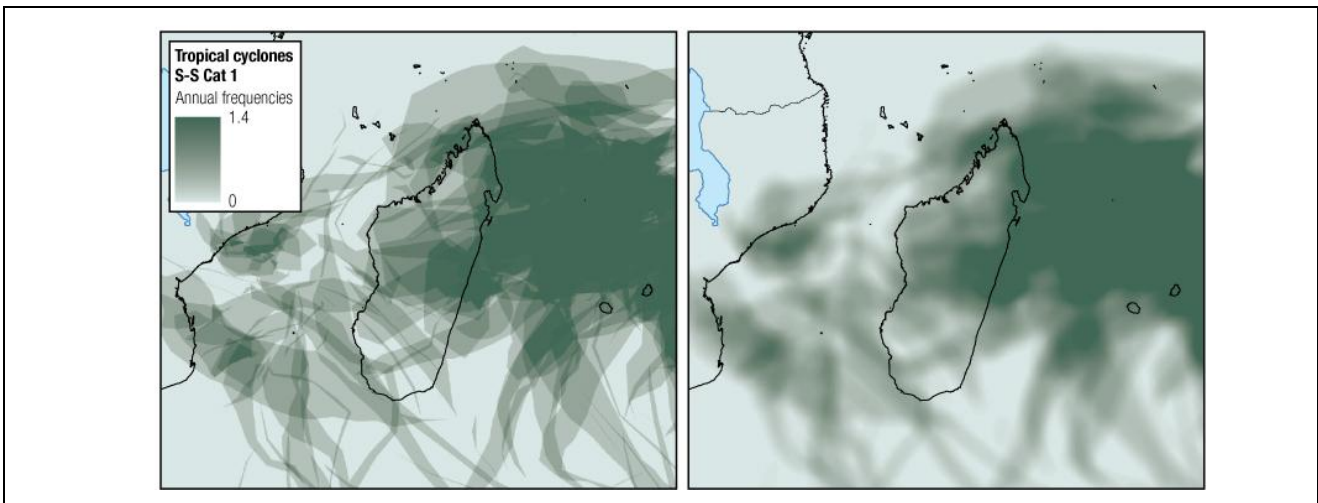
The severity of the cyclone hazard over the total period of analysis has been taken into account by averaging the sum of wind that affected annually each pixel of a grid for all Saffir-Simpson categories (see Figure 1).

### *From windspeed buffers to frequencies*

Finally annual frequency grids have been processed for each Saffir-Simpson categories by summing the number of time each pixel has been affected by a given Saffir-Simpson category and dividing the total by the length of the dataset period.

Fuzziness of the limits between Saffir-Simpson categories as well as the accuracy of the best track coordinates and simulation has been included in the frequencies grid by smoothing the raw grid (see Figure 6).

**Figure 6 Tropical cyclone frequencies: raw in the left, smoothed in the right**



### *Difficulties and limitations*

The absence of an official format for archiving tropical cyclone events complicated the compilation of a global data set. Even if special attention has been given to this process, missing or duplicate events remain possible.

The 2D model developed by GRID-Europe remains only valid on the ocean and becomes uncertain as soon as landfall happens. As a consequence the exposed area has been restricted to a 200 km band along the coastline. Even with this restriction, deep inland data has to be interpreted carefully.

### *Next steps*

The allocation of victims or damages across the different wind categories remains a big uncertainty of the risk modelling. To improve this process, a feasibility study could be performed by combining the present models with available local high resolution damage data sets.

The two existing models (wind, surge) could be combined, and a precipitation factor could be included in order to get a full idea of this complex hazard. Again the allocation of victims within the two factors should be clarified.

## **1.3. References**

### *Articles and books*

Bell, G. D., and Chelliah, M, 2006: Leading Tropical Modes Associated with Interannual and Multidecadal Fluctuations in North Atlantic Hurricane Activity, *Journal of Climate* 19(4), 590-612.

Chan, J. C. L., 2006: Comment on "Changes in Tropical Cyclone Number, Duration, and Intensity in a Warming Environment", *Science*, 311, 1713b.

Dao H., Peduzzi P. (2004), Global evaluation of human risk and vulnerability to natural hazards, *EnviroInfo 2004 Proceedings*, Geneva.

Emanuel, K., 2005: Increasing destructiveness of tropical cyclones over the past 30 years, *Nature*, 436 (4), 686-688.

Holland, G. J., (1980). An analytic model of the wind and pressure profiles in hurricanes. *Monthly Weather Review*, 108, pp. 1212-1218.

IWTC06, 2006: Statement on Tropical Cyclones and Climate Change, WMO International Workshop on Tropical Cyclones, San Jose, Costa Rica.

McTaggart-Cowan, Ron; Lance F. Bosart, Christopher A. Davis, Eyad H. Atallah, John R. Gyakum, and Kerry A. Emanuel (November 2006). "Analysis of Hurricane Catarina (2004)", *Monthly Weather Review* **134** (11): 3029–3053, doi:10.1175/MWR3330.1.

Marcelino, Emerson Vieira; Isabela Pena Viana de Oliveira Marcelino; Frederico de Moraes Rudorff (2004). "Cyclone Catarina: Damage and Vulnerability Assessment", Santa Catarina Federal University, [http://www.dsr.inpe.br/geu/Rel\\_projetos/Relatorio\\_IAI\\_Emerson\\_Marcelino.pdf](http://www.dsr.inpe.br/geu/Rel_projetos/Relatorio_IAI_Emerson_Marcelino.pdf)

Nordbeck, O., Mouton, F., Peduzzi, P. (2005). Cyclone Data Manager: A tool for converting point data from cyclones observations into tracks and windspeed profiles in a GIS. UNEP/GRID-Europe. [www.grid.unep.ch/product/publication/download/article\\_PREVIEW\\_TropCyclones.pdf](http://www.grid.unep.ch/product/publication/download/article_PREVIEW_TropCyclones.pdf)

Peduzzi, P., Dao, H., Herold, C., Mouton, F., (2002), Global Risk And Vulnerability Index Trends per Year (GRAVITY), phase II: Development, analysis and results. 56 p. (Technical document, not yet public).

Pezza, Alexandre B.; Ian Simmonds (April 2006). "Catarina: The First South Atlantic Hurricane and its Association with Vertical Wind Shear and High Latitude Blocking". Proceedings of the 8th International Conference on Southern Hemisphere Meteorology and Oceanography: 353-364, Foz do Iguaçu, Brazil: Instituto Nacional de Pesquisas Espaciais.

Schloemer, R.W. (1954). Analysis and synthesis of hurricane wind patterns over Lake Okechoe, FL. Hydromet Rep. 31, 49 pp. [Govt. Printing Office, No. C30.70:31].

UNDP (2004). Reducing disaster risk: a challenge pour development, United Nations Development Programme

Bureau for Crisis Prevention and Recovery, 146 p.

#### *Internet references*

Global Risk Data Platform: <http://preview.grid.unep.ch>)

#### *Data sources*

This new study would not have been possible without the collaboration of all the WMO Regional Specialised Meteorological Centres (RSMCs) and Tropical Cyclone Warning Centres (TCWCs) who are the providers of the best tracks data collection. Without the raw data none of the following products could have been derived. Hence we are very grateful to Dr. Varigonda Subrahmanyam, Dr. James Weyman, Kiichi Sasaki, Philippe CAROFF, Jim Davidson, Simon Mc Gree, Steve Ready, Peter Kreft, Henrike Brecht and all the persons that have contributed to provide the raw data. We also would like to thank Nanette Lomarda (WMO) for facilitating the contacts.

## 2. Floods

### 2.1. Authors

#### *Hazard Model*

Christian Herold (UNEP/GRID-Europe)

Dr. Frédéric Mouton, (University of Grenoble, Institut Fourier )

Contributors: Code for flooded area model provided by Jim & Kristin Verdin (USGS)

#### *Flood events*

Christian Herold (UNEP/GRID-Europe)

With major contribution from: Robert Brackenridge (Dartmouth Flood Observatory, DFO)

#### *Floods expert group*

Kristin Verdin (USGS)

James Verdin, (USGS)

Robert Brackenridge (DFO)

Wolfgang Grabs (Hydrology and Water Resources Programme, WMO)

#### *Hazard methodology reviewed by:*

Zhiyu LIU, P.E. (Deputy Director, Division of Hydrological Information and Forecasting, Bureau of Hydrology (National Flood Forecasting Center), Ministry of Water Resources of China.

#### *Focal points at WMO Secretariat:*

Avinash Tyagi, (Director, Climate and Water Department and Chief, Hydrology and Water Resources Programme, WMO)

Wolfgang Grabs (Hydrology and Water Resources Programme, WMO)

### 2.2. Hazard

Floods are one of the most frequent natural hazards and occur in almost every country. A flood is generally defined as an excess of the amount of discharged water compared to the drainage capacity. At present there is no systematic global detection of flood events as there is for cyclones and earthquakes.

Floods are triggered by various phenomena and there are different types of floods. For example one often differentiates among flash floods, river floods, and urban floods, all of which are caused by a combination of heavy precipitation and poor drainage. The severity of these flood types depends on rainfall intensity, spatial distribution of rainfall, topography and surface conditions.

All coastal areas are vulnerable to flood events, which could be devastating when heavy rainfall occurs at the same time as high tide or storm surge. Many climate change models predict more frequent extreme precipitation events, which in combination with global sea level rise makes the situation even more critical in the future. Consequently, the risk associated with flooding is expected to increase significantly in coastal regions with high population density in the future. Because of the predictability of the flooding events, however, the main consequences will usually be damage to constructed facilities and discomfort of the exposed population, rather than loss of life.

#### *Modelling flood*

The current study focused on river floods. Other flooding events are not caused by precipitation, e.g. coastal flooding tends to be associated with atmospheric low pressure systems driving ocean water inland. Glacial lake outburst flooding (GLOF) occurs when a terminal or lateral moraine fails, releasing the glacial melt water it was damming in a sudden, violent burst. These flood types would require different modelling than what was done in the present study. Coastal flooding was, however, included in the modelling of storm surge during tropical cyclones (see Chapter 1).

Peak-flow magnitude estimates for ungauged sites have been computed, based on records from a set of gauging stations, following the directions of the Bulletin 17B from United States Water Resources Council's Hydrology Subcommittee: "Guidelines for determining flood flow frequency" and the Water-Resources Investigation Report 98-4055: "Techniques for Estimating Peak-Flow Magnitude and Frequency Relations for South Dakota Streams" by Steven K. Sando.

This is a four-step process: estimation of peak-flow values for a hundred-year recurrence interval for gauging stations, based on log-Pearson type III modelling of the records; constitution of groups of gauging stations taking into account basin and climatic characteristics; elaboration of a regression formula for each group, which predicts peak-flow values from basin and climatic characteristics; attribution of a reference group for each ungauged site and estimation of its peak-flow by the corresponding regression formula.

In order to solve the problem of data homogeneity in some climatic regions, a global approach is adopted for the whole statistical analysis.

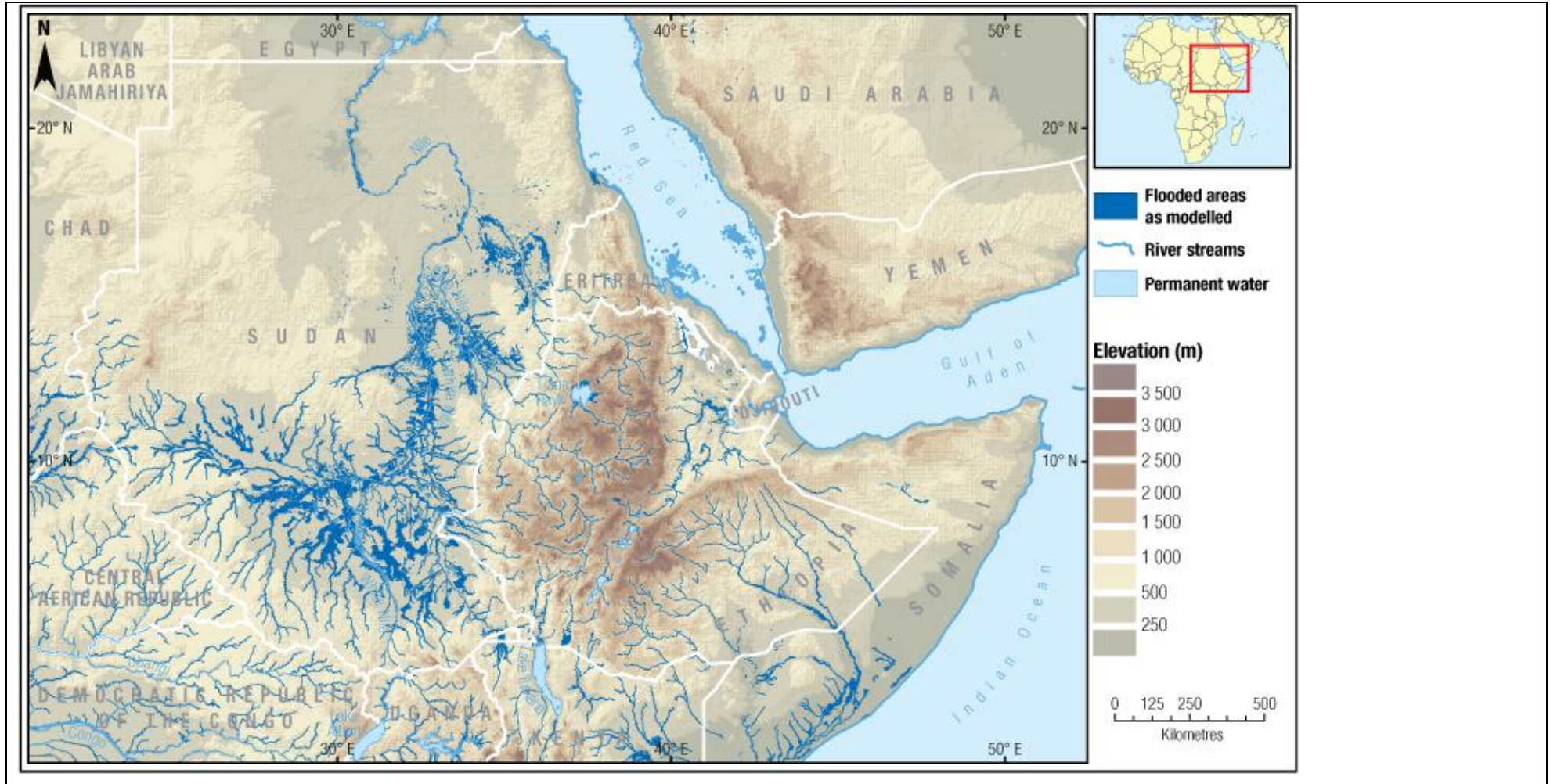
Flooded areas corresponding to exceptional events of a hundred-year recurrence interval are generated by calculation of river stage. This is achieved using peak-flow estimates and Manning equation through complex and automated processes based on Georeferenced Information System.

The simulated intensity corresponds to a hundred-year return period event. Given that smaller events are very likely to occur, a model based only on one return period is not sufficient. However, given the limited amount of time and the extensive demand of computation (months of computing time), it was not possible to generate several return period. To overcome this issue, the frequency was obtained by multiplying the frequency file by the UNEP/GRID-Europe PREVIEW flood frequency. This frequency was based on recorded flooded watersheds between 1980 and 2001 (21 years). The resolution was really poor given that only the boundaries of the watersheds flooded were recorded, not the actual flood extents. However, the frequency can still be multiplied by the much more precise river flooding model. When no frequency was recorded for a selected area, it was replaced arbitrarily by 0.02, i.e. 2 events in 100 years to account for the smaller surfaces that might be flooded before. This is not satisfactory, however, most of the areas are covered by PREVIEW flood frequency.

#### *Observed flood events*

In addition to modelled floods, nine years of actual flood events, as detected by satellite from Dartmouth Flood Observatory (DFO), were incorporated. The observed flooding events, based mostly on MODIS satellite sensors at 250 m resolution, provided additional information and were also used for calibration. The data for observed flood events cover only nine years, containing more than 400 events and are not comprehensive. The combination of observed and modelled datasets provides a good picture of the most flood-prone areas.

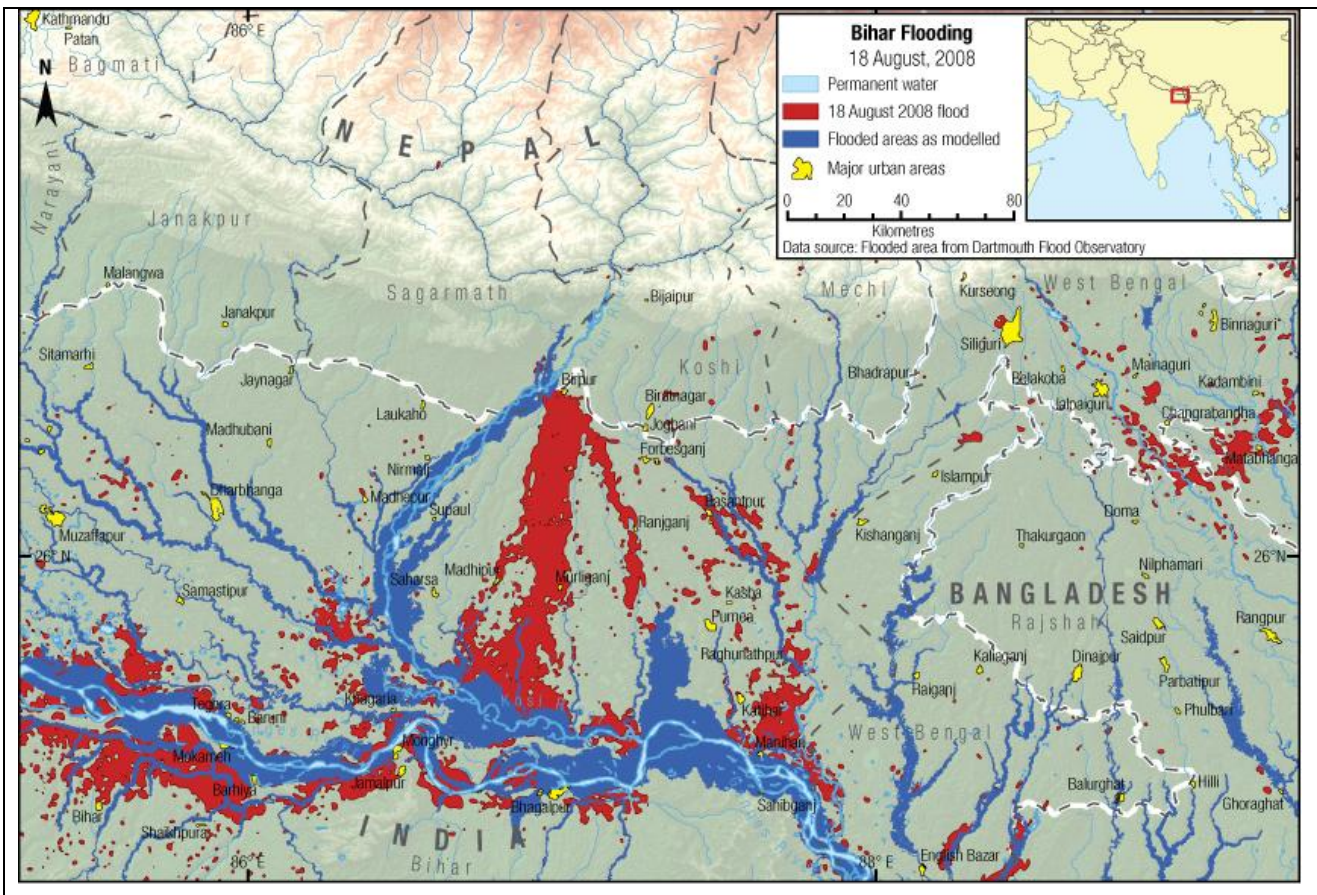
Figure 7 Map showing flood hazard distribution for East part of Africa



*Difficulties and limitations*

Figure 8 shows the simulated and observed flood in the Bihar region in August 2008. This flood has affected 3.3 million people in 1,598 villages located in 15 districts, and killed 47 people (EM-DAT). It was caused by a broken dike, an event that could not be predicted by the flood model used in this analysis. This tragedy sadly demonstrates that the global models provided in this research SHOULD NOT be used for local planning. Global models have only the purpose of identifying areas where more research should be conducted. The model cannot take into consideration the solidity of a dike or local scale topographical features, although a tremendous improvement was made with elevation data set, they are still dedicated to be used at a global level. Unexpected events such as the 18th August 2008 and others cannot be forecasted, without a local engineered study.

**Figure 8 Map of model with the Bihar flood 2008**



## 2.3. References

### Articles and books

- Bravard, J.-P., Petit, F., 2000, Les cours d'eau, Dynamique du système fluvial.
- Chow, V. T., Maidment, D. R., Mays, L. W., 1988, Applied Hydrology.
- Farquharson, F.A.K., J.R. Meigh, and J.V. Sutcliffe, 1992. Regional flood frequency analysis in arid and semi-arid areas. *Journal of Hydrology* 138:487-501.
- Kachroo, R.K., S.H. Mkhandi, and B.P. Parida, 2000. Flood frequency analysis of southern Africa: I. Delineation of homogeneous regions. *Hydrological Sciences*, 45 (3) 437-447.
- Katz, R.W., M.B. Parlange, and P. Naveau, 2002. Statistics of extremes in hydrology. *Advances in Water Resources* 25: 1287-1304.
- Kjeldsen, T.R., J.C. Smithers, and R.E. Schulze, 2001. Flood frequency analysis at ungauged sites in the Kwazulu-Natal Province, South Africa. *Water SA* Vol. 27, No.3, pp.315-324. , <http://www.wrc.org.za>.
- McGregor, G.R., 1990. Application of regional flood frequency analysis to large tropical catchments: A case study in the Sepik Basin, Papua, New Guinea, *Singapore Journal of Tropical Geography*, Vol. 11, No. 1, pp.1- 12.
- Meigh, J.R., F.A.K. Farquharson, and J.V. Sutcliffe, 1997. A worldwide comparison of regional flood estimation methods and climate. *Hydrological Sciences* 42(2): 225-244.
- Mkhandi, S. H., Kachroo, R. K. & Gunasekara, T. A. G. (2000) Flood frequency analysis of southern Africa: II. Identification of regional distributions. *Hydrol. Sci. J.* 45(3), 449-466.
- Musy, A., Soutter, M., 1991, Physique du sol.
- Musy, A., 2005, Hydrologie générale. <http://hydram.epfl.ch/e-drologie/>.
- Sando, S. K., Water-Resources Investigation Report 98-4055: Techniques for Estimating Peak-Flow Magnitude and Frequency Relations for South Dakota Streams.
- Topaloglu, F., 2005. Regional flood frequency analysis of the basins of the East Mediterranean Region. *Turk J Agric For* 29: 287-295.
- United States Water Resources Council's Hydrology Subcommittee, 1982, Bulletin 17B: Guidelines for determining flood flow frequency.
- K.L. Verdin, J.P. Verdin, 1999, A topological system for delineation and codification of Earth's river basins.

## 2.4. Data sources

- Long-term mean monthly discharge dataset. The Global Runoff Data Centre (GRDC), 56002 Koblenz, Germany.
- R-ArcticNET, A Regional, Electronic, Hydrographic Data Network For the Arctic Region. Water Systems Analysis Group. Complex Systems Research Center. Institute for the Study of Earth, Oceans and Space. University of New Hampshire.
- The Global River Discharge Database (RivDIS v1.1). Water Systems Analysis Group. Complex Systems Research Center. Institute for the Study of Earth, Oceans and Space. University of New Hampshire.
- Monthly Discharge Data for World Rivers (except former Soviet Union). DE/FIH/GRDC and UNESCO/IHP, 2001: Monthly Discharge Data for World Rivers (except former Soviet Union). Published by the CISL Data Support Section at the National Center for Atmospheric Research, Boulder, CO (ds552.1). <http://dss.ucar.edu/datasets/ds552.1/>
- Russian River Flow Data by Bodo, Enhanced. Monthly river flow rates for Russia and former Soviet Union countries in ds553.1 are augmented with data from Russia's State Hydrological Institute (SHI) and a few sites from the Global Hydroclimatic Data Network (GHCDN).
- Discharge of selected rivers of the world. World Water Resources and their use, a joint SHI/UNESCO product. International Hydrological Programme. UNESCO's intergovernmental scientific programme in water resources.
- HYDRO1k Elevation Derivative Database. EROS, USGS.
- HydroSHEDS, WWF. In partnership with USGS, CIAT, TNC, CESR.
- Global Drainage Basin Database (GDBD). Yuji Masutomi, Yusuke Inui, Kiyoshi Takahashi, and Yuzuru Matsuoka (2007) Development of highly accurate global polygonal drainage basin data. Submitted to *Hydrological Processes*.
- Global land cover GLC\_2000 version 1. Institute for Environment and Sustainability, Joint Research Centre. <http://www-gvm.jrc.it/glc2000/>
- Global Lakes and Wetlands Database (GLWD). Lehner, B. and Döll, P. (2004): Development and validation of a global database of lakes, reservoirs and wetlands. *Journal of Hydrology* 296/1-4: 1-22. <http://www.wwfus.org/science/data/globallakes.cfm>
- CRU TS 2.1 monthly precipitation. Mitchell, T.D., 2004: An improved method of constructing a database of monthly climate observations and associated high resolution grids.

CRU TS 2.1 monthly mean temperatures. Mitchell, T.D., 2004: An improved method of constructing a database of monthly climate observations and associated high resolution grids.

Variability Analyses of Surface Climate Observations (VASCLimO) at the Global Precipitation Climatology Centre (GPCC). Version-1.1, 0.5°x0.5°. Beck, C., J. Grieser and B. Rudolf (2005): A New Monthly Precipitation Climatology for the Global Land Areas for the Period 1951 to 2000, Climate Status Report 2004, pp. 181 - 190, German Weather Service, Offenbach, Germany.

World Map of the Köppen-Geiger climate classification updated. Kottek, M., J. Grieser, C. Beck, B. Rudolf, and F. Rubel, 2006: World Map of the Köppen-Geiger climate classification updated. Meteorol. Z., 15, 259-263. University of Veterinary Medicine Vienna.

Updated world map of the Köppen-Geiger climate classification. Peel MC, Finlayson BL & McMahon TA (2007), Updated world map of the Köppen-Geiger climate classification, Hydrol. Earth Syst. Sci., 11, 1633-1644. The University of Melbourne, Victoria, Australia.

The Holdridge Life Zones data set. Leemans, Rik, 1990. Global data sets collected and compiled by the Biosphere Project, Working Paper, IIASA-Laxenburg, Austria.

World Atlas of Flooded Lands. Dr. G. Robert Brakenridge, Ms. Elaine Anderson. Dartmouth Flood Observatory.

PREVIEW Flood Frequency: UNEP/DEWA/GRID-Europe Georeference from CRED for the project GRAVITY  
P. Peduzzi, H. Dao, C. Herold, B. Widmer, T. Ton That, A. Martin-Diaz (2002), [http://www.grid.unep.ch/activities/earlywarning/preview/data/floods/index\\_flood.php](http://www.grid.unep.ch/activities/earlywarning/preview/data/floods/index_flood.php)

### 3. Drought

#### 3.1. Authors

*Hazard Model (Columbia University)*

Brad Lyon (IRI, Columbia University)

Gregory Yetman (CIESIN, Columbia University)

Maria Muniz (CIESIN, Columbia University)

Liana Razafindrazay Research Associate at CIESIN – Columbia University

Vilentia Mara from CIESIN, Columbia University.

*Hazard methodology reviewed by:*

Simone Orlandini (Prof., Department of Agronomy and Land Management - University of Florence)

Harlan D. Shannon (Meteorologist, U.S. Department of Agriculture World Agricultural Outlook Board)

Mark Svoboda (Climatologist, National Drought Mitigation Center, School of Natural Resources, University of Nebraska-Lincoln)

Orivaldo BRUNINI (Instituto Agronomico, SAO PAULO, Brazil)

*Focal points in WMO Secretariat:*

Mannava Sivakumar (Chief, Agricultural Meteorology Programme, WMO)

Robert Stefanski (Agricultural Meteorology Programme, WMO)

#### 3.2. Hazard

Drought is a phenomenon that affects more people globally than any other natural hazard. Unlike aridity, which refers to a semi-permanent condition of low precipitation (desert regions), drought results from the accumulated effect of deficient precipitation over a prolonged period of time. Here “deficient” refers to values being less than the expected, or long-term average value at a particular location. Ultimately, drought refers to a condition of an insufficient supply of water necessary to meet demand, both being highly location-specific. For example, a few months of deficient rainfall can adversely affect rain-fed agricultural systems while several months to a year (or more) of drought may be necessary to impact a water supply system with substantial storage capacity. Given the varying impacts of drought several drought indicators are in use around the world.

Drought is often described as falling into three main categories: meteorological, agricultural, and hydrologic. Meteorological drought refers to a prolonged period of deficient precipitation that may last from a season to several years. Agricultural drought occurs when soil moisture is depleted to the point where it begins to adversely affect crops, pasture, or rangeland. A reduction in soil moisture is in part related to precipitation but also depends on other meteorological conditions such as temperature and wind as well as non meteorological factors such as soil type and terrain. Hydrologic drought refers to a condition of persistent, below-average surface water levels in rivers, streams, lakes and reservoirs or subsurface water such as an unusually low water table. These conditions are again partially related to precipitation variability but also to non-meteorological factors. Given the importance of non-meteorological factors, there is often a delay between the onset of meteorological drought and agricultural or hydrologic drought. The “best” indicator for drought is the one that most closely corresponds to the specific drought-sensitive application being considered.

Among natural hazards, drought risk is especially difficult to quantify. First, unlike earthquakes, floods or tsunamis that occur along generally well-defined fault lines, river valleys or coastlines, drought can occur anywhere (with the exception of deserts where it doesn't have meaning). Defining what constitutes a drought across the wide range of regional climates around the globe is challenging in its own right, identifying what drought characteristic (its intensity, duration, spatial extent) is most relevant to a specific drought sensitive sector (agriculture, water management, etc.) poses another layer of complexity. Drought does not destroy infrastructure or directly lead to human mortality. Famines may be triggered by drought but increased human mortality during famine is ultimately linked to a broader set of issues surrounding food security.

#### *Modelling droughts*

To be applicable across varying climate regions of the globe the approach in the current study is to look at standardized drought indices. Standardizing allows variations in drought index values to be viewed on a common scale across regions with varying climates. Specifically, we examine the Standardized Precipitation Index (SPI; McKee et al. 1993). The SPI compares an accumulated precipitation amount for a given time interval (in the present study the past 3, 6 and 12 months over the period 1951-2004) with historical values for the same month. The difference between the observed and historical value is then expressed in terms of a standardized normal distribution having a mean of zero (indicating no difference

from the historical average). Increasingly negative values of the SPI indicate increasingly drier-than-average conditions, with values less than -1 generally considered to indicate drought (Figure 9).

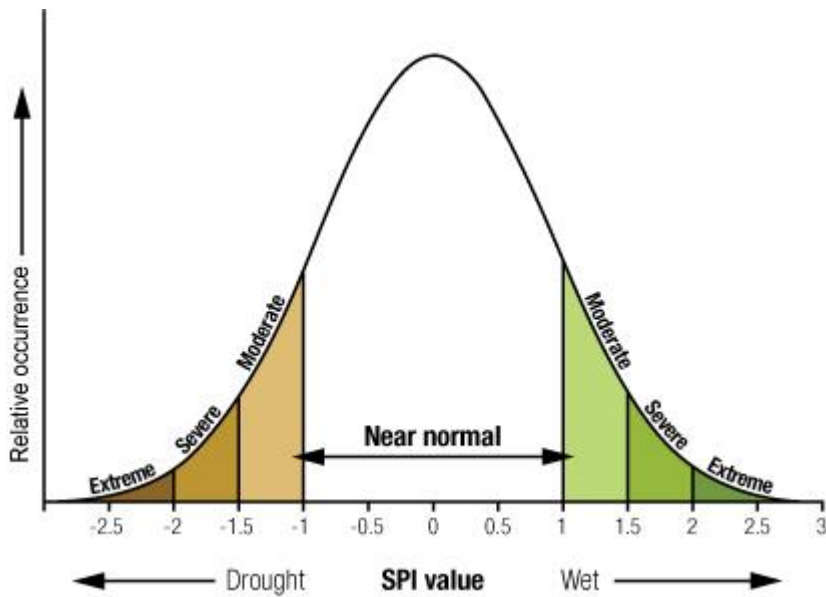


**Figure 9** *The relative occurrence versus value of the SPI. Index values < -1.0 are associated with drought conditions.*

To examine the relative occurrence of drought “events” across the globe, run statistics drought indices were assessed. This analysis was performed at the grid point level and runs in the SPI time series, when index values fell below different truncation levels (in the present study -1.0 and -1.5), were evaluated. This approach is widely used in the analysis of hydro meteorological time series and drought frequency analysis (Dracup et al. 1980; Clausen and Pearson 1995; Fernández and Salas 1999; Keyantash and Dracup 2002; Sirdaş and Şen 2004; among many others).

Figure 10 Global distribution of drought frequency

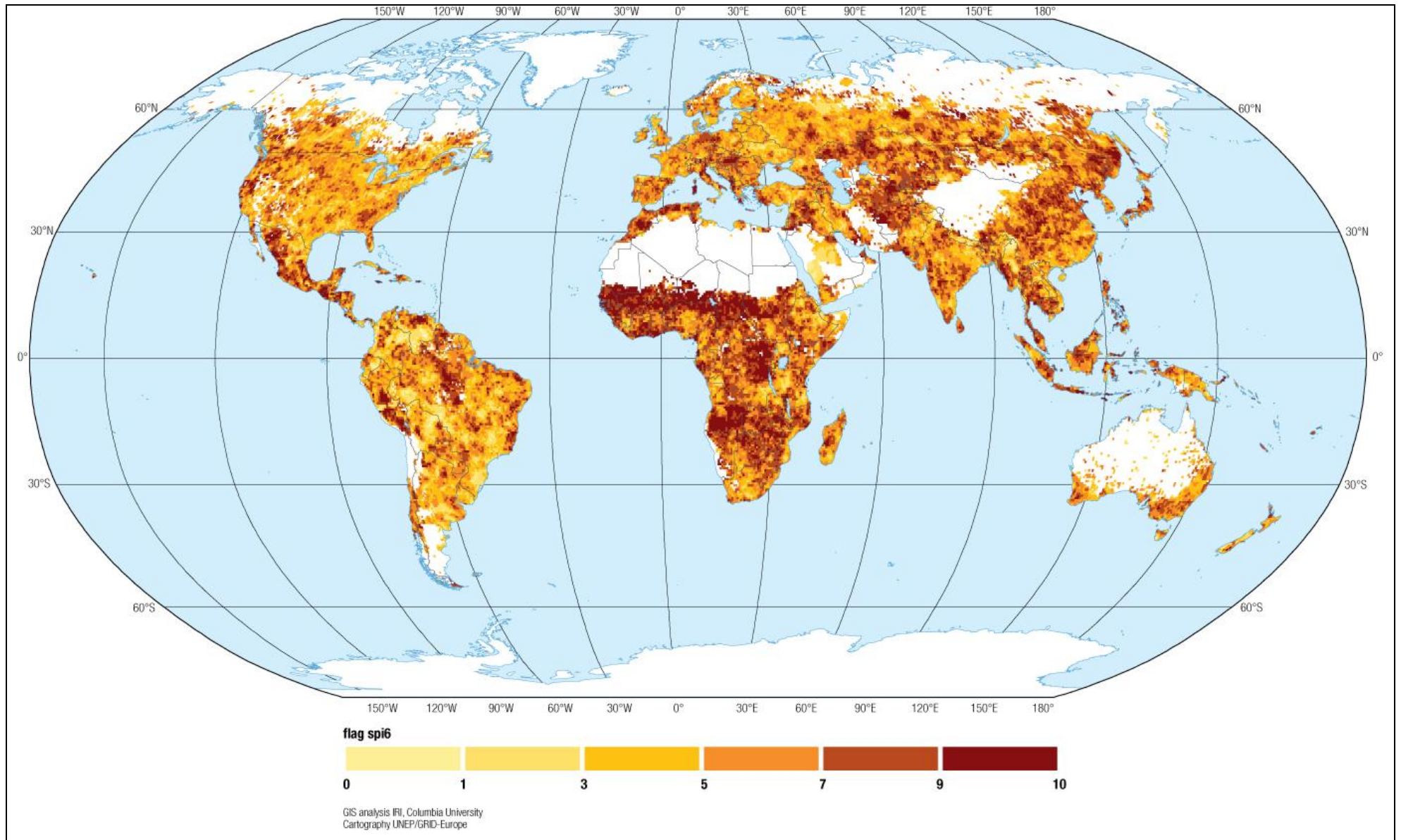
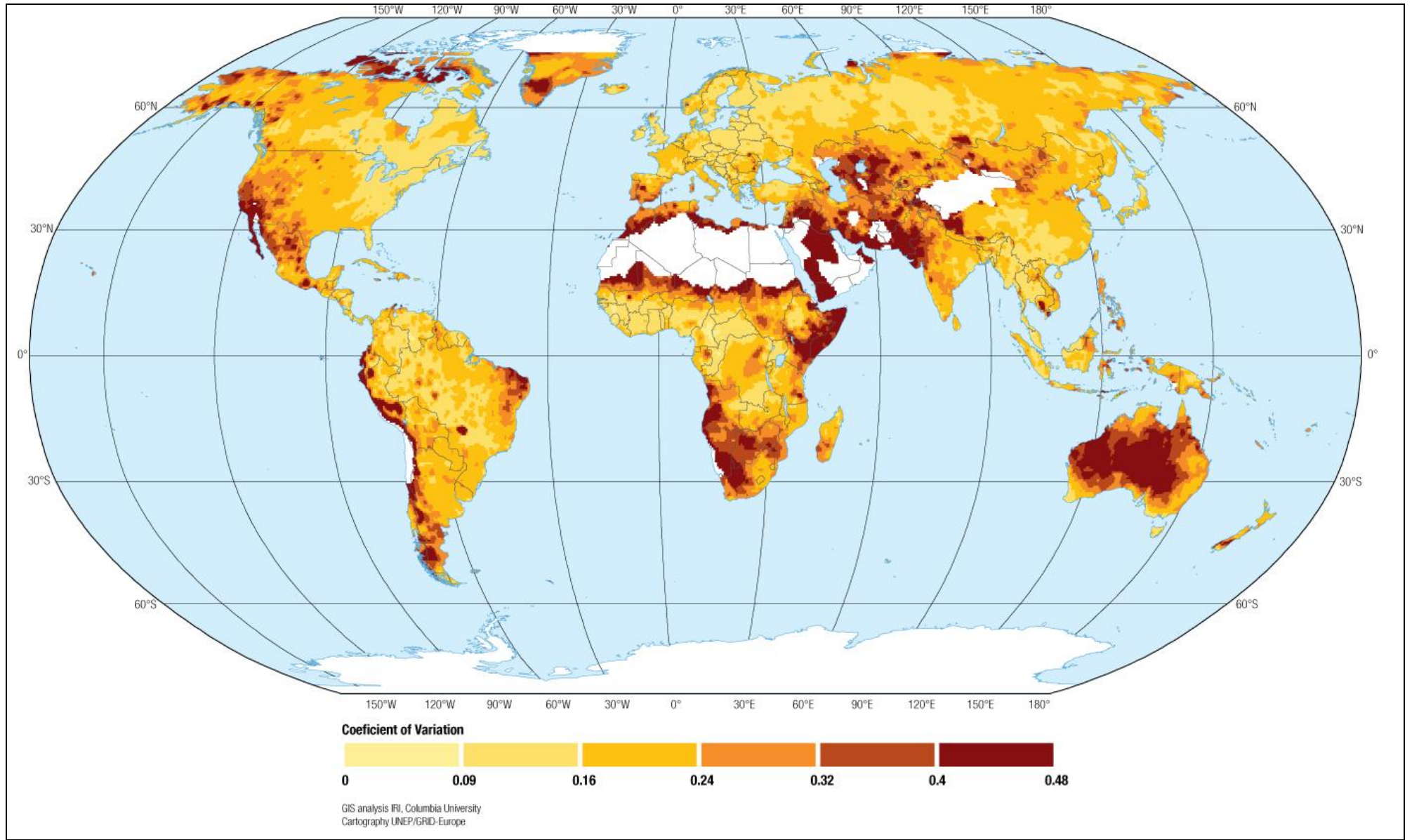


Figure 11 Global distribution of Coefficient Variation (1970-2000)



In addition to the SPI, a coefficient of variation (CV) was computed. The CV gives an additional bit of information since it is a summary measure (that is, a single value for a 30-year period) of how large the variability of precipitation is from year-to-year, relative to the amount of mean annual rainfall.

Drought intensity and frequency are captured by the SPI. The CV gives additional information since it is a summary measure (that is, a single value for a 30-year period) of how large the variability of precipitation is from year-to-year, relative to the amount of mean annual rainfall. This is why the CV tends to be high in semi-arid regions: there tends to be both high variability of rainfall in regions with small mean annual rainfall.

To place more emphasis on areas having already a low amount of precipitation, the maps on drought hazard was obtained by multiplying the SPI-defined drought event frequency by the CV therefore combining drought intensity, frequency and information on where inter-annual precipitation variability is high (or low).

*However for the computation of physical exposure, only SPI was used.*

#### *Difficulties and limitations*

The global scale analysis undertaken in this study has some important limitations. First, variations in regional climate which are associated with small scale topographic features, such as rain shadows, will likely not be well captured in the drought analysis. More generally, the issue of data quality in regions with sparse precipitation observing stations needs to be kept in mind. Using the calendar year as the period in which drought events are identified may obfuscate the occurrence of events that develop near the start, or end, of a given year.

Since the EM-DAT data typically contains disaster information for only the most severe drought cases the sample size can be quite limited for many countries making robust statistical comparisons impossible for an individual country.

#### *Next steps*

Hydrologic modelling is advancing rapidly and global analyses of several output variables (estimated soil moisture, runoff, evaporation) are being developed for estimating historical conditions and in real time monitoring. While there are caveats concerning the calibration of these models they provide information at fairly high spatial resolution and represent the next generation products. In future efforts these data can be compared with precipitation-based drought indices and with drought impacts reports. Drought impacts research can also be advanced through case studies where sufficient high quality and high resolution data exist. The potential effect of global warming on the physical characteristics of drought (intensity, duration, spatial extent) represents another important area of research that clearly has implications for human impacts.

### **3.3. References**

#### *Articles and books*

Barlow, M., H. Cullen, B. Lyon, and O. Wilhelmi, 2004: Drought Disaster in Asia. In *Natural Disaster Hotspots Case Studies*, International Bank for Reconstruction and Development/The World Bank and Columbia University, Washington, DC p. 1-19.

Clausen, B. and C.P. Pearson, 1995: Regional frequency analysis of annual maximum streamflow drought. *Journal of Hydrology*, 173, 111-130.

Dilley, M., R.S. Chen, U. Deichmann, A.L. Lerner-Lam, M. Arnold, J. Agwe, P. Buys, O. Kjekstad, B. Lyon, and G. Yetman, 2005: *Global Natural Disaster Hotspots*. International Bank for Reconstruction and Development/The World Bank and Columbia University, Washington, DC and New York. 132 pp.

Dracup, J.A., K.S. Lee, and E.G. Paulson, Jr., 1980: On the Definition of Droughts. *Water Resources Research*, 16(2), 297-302.

Fan Y., H. van den Dool (2004), Climate Prediction Center global monthly soil moisture data set at 0.5° resolution for 1948 to present, *J. Geophys. Res.*, 109, D10102, doi:10.1029/2003JD004345.

Fernández, B. and J.D. Salas, 1999: Return Period and Risk of Hydrological Events. II: Applications. *Journal of Hydrologic Engineering*, 4, 308-316.

Hayes. M.J., M. Svoboda, D. Le Comte, K.T. Redmond, and P. Pasteris, 2005: Drought Monitoring: New Tools for the 21st Century. In *Drought and Water Crises: Science, Technology, and Management Issues*, 2005, D.A. Wilhite, Ed., Taylor and Francis, Boca Raton, FL, 406 pp.

Keyantash, J. and J.A. Dracup, 2002: *The Quantification of Drought: An Evaluation of Drought Indices*.

Lyon, B., L. Zubair, V. Ralapanawe, and Z. Yahiya, 2008: Fine-scale evaluation of drought hazard for tropical climates: Case study in Sri Lanka. *Journal of Applied Meteorology and Climatology* (in press).

Mckee, T.B., N.J. Doesken, and J. Kleist, 1993: The relationship of drought frequency and duration to time scales. *Proceedings of the 8th Conference on Applied Climatology*, p. 179-184, Anaheim, CA.

Wilhite, D.A., and M. Buchanan-Smith, 2005: Drought as Hazard: Understanding the Natural and Social Context. In *Drought and Water Crises: Science, Technology, and Management Issues*, 2005, D.A. Wilhite, Ed., Taylor and Francis, Boca Raton, FL, p. 3-29.

Wilhite, D.A., 2005: *Drought and Water Crises: Science, Technology, and Management Issues*, Ed., Taylor and Francis, Boca Raton, FL, 406 pp.

#### *Internet references*

Early Warning Systems for Drought Preparedness and Drought Management. Workshop summary from the US Drought Mitigation Center, University of Nebraska, Lincoln:  
[http://drought.unl.edu/monitor/EWS/EWS\\_WMO.html](http://drought.unl.edu/monitor/EWS/EWS_WMO.html)

#### **3.4. Data sources**

Precipitation Data: Monthly, gridded precipitation analyses for the globe were obtained from the Global Precipitation Climatology Center (GPCC). These analyses are based on station observations which have been spatially interpolated to generate gridded analyses at a 0.5 x 0.5 deg. lat/long resolution. The available data covered the period Jan 1951 to Dec 2004. Although gridded to a nominal 0.5 x 0.5 deg. lat/lon. grid, the precipitation analyses are likely to contain larger errors in data sparse regions. Another caveat in using these data in the context of precipitation-only drought indices such as the SPI is that other parts of the surface water balance such as infiltration, runoff, and evaporation are not considered.

## 4. Landslides

### 4.1. Authors

*Hazard model* (International Centre for Geohazards / NGI)

Helge Smebye

Bjørn Kalsnes

*Hazard methodology reviewed by:*

Kyoji Sassa (University of Kyoto, Japan; President of ICL)

Nicola Casagli (University of Firenze, Italy; Director of ICL-Europe)

Lynn Highland (United States Geological Survey, USA)

Dwikorita Karnawati (Associate Professor, Gadjah Mada University, Indonesia)

Alexander Strom (Institute of the Geospheres Dynamics, Russia, Assistant to the ICL President)

### 4.2. Hazard

The term landslide in this report refers to slides with rapid mass movement, like rockslides, debris flows, induced by both rainfall and earthquake; which pose a threat to human life. Slow moving slides have significant economic consequences for constructions and infrastructure, but rarely cause any fatalities. Rapid mass movement also includes snow avalanche, this later is not covered in this report, as well as rock avalanches and submarine slides.

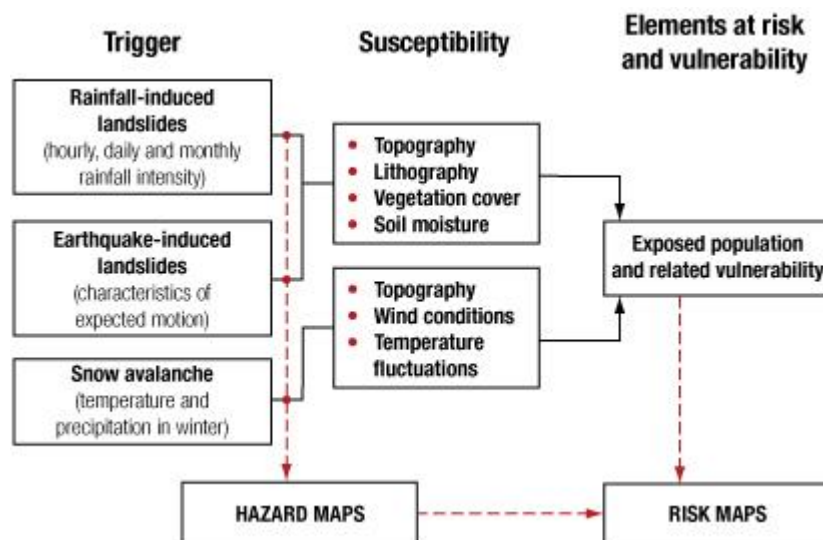
Landslides represent a major threat to human life, property and constructed facilities, infrastructure and natural environment in most mountainous and hilly regions of the world. Statistics from the Centre for Research on the Epidemiology of Disasters (CRED) show that, on average, landslides are responsible for a small fraction of all fatalities from natural hazards worldwide. The socio-economic impact of landslides is, however, greatly underestimated because landslides are usually not separated from other natural hazard triggers, such as extreme precipitation, earthquakes or floods in natural catastrophe databases. This underestimation contributes to reducing the awareness and concern of both authorities and general public about landslide risk.

Only the population exposure to precipitation-induced landslides was considered in the event-per-event analysis. The fatalities caused by earthquake-induced landslides are attributed to “earthquakes” in the EM-DAT database, and including them again under “landslides” would lead to an overestimation of risk.

#### *Modelling landslides*

The landslide hazard, defined as the annual probability of occurrence of a potentially destructive landslide event, depends on the combination of trigger and susceptibility (Figure 12). In the analyses performed in this study, a landslide hazard index was defined using six parameters: slope factor, lithological (or geological) conditions, soil moisture condition, vegetation cover, precipitation and seismic conditions.

**Figure 12. Schematic approach for landslide hazard and risk evaluation.**



For each factor, an index of influence was determined and a relative landslide hazard indicator was obtained by multiplying and summing the indices.

The obtained landslide hazard indices were calibrated against the databases of landslide events in selected (mostly European) countries to obtain the frequency of the events.

**Table 2 Landslide hazards frequencies and severity**

<b>Category</b>	<b>Frequencies</b>	<b>Proportion</b>	<b>Annual surface / km2</b>
<b>Low to Moderate</b>	0.01%	5%	0.000005
<b>Low to Moderate</b>	0.03%	5%	0.000015
<b>Moderate</b>	0.10%	5%	0.000050
<b>Medium to High</b>	0.30%	7%	0.000210
<b>Medium to High</b>	1%	9%	0.000900
<b>High</b>	3%	12%	0.003600
<b>Very High</b>	10%	15%	0.015000

**Figure 13 Map of Precipitation triggered Landslides Hazard distribution**

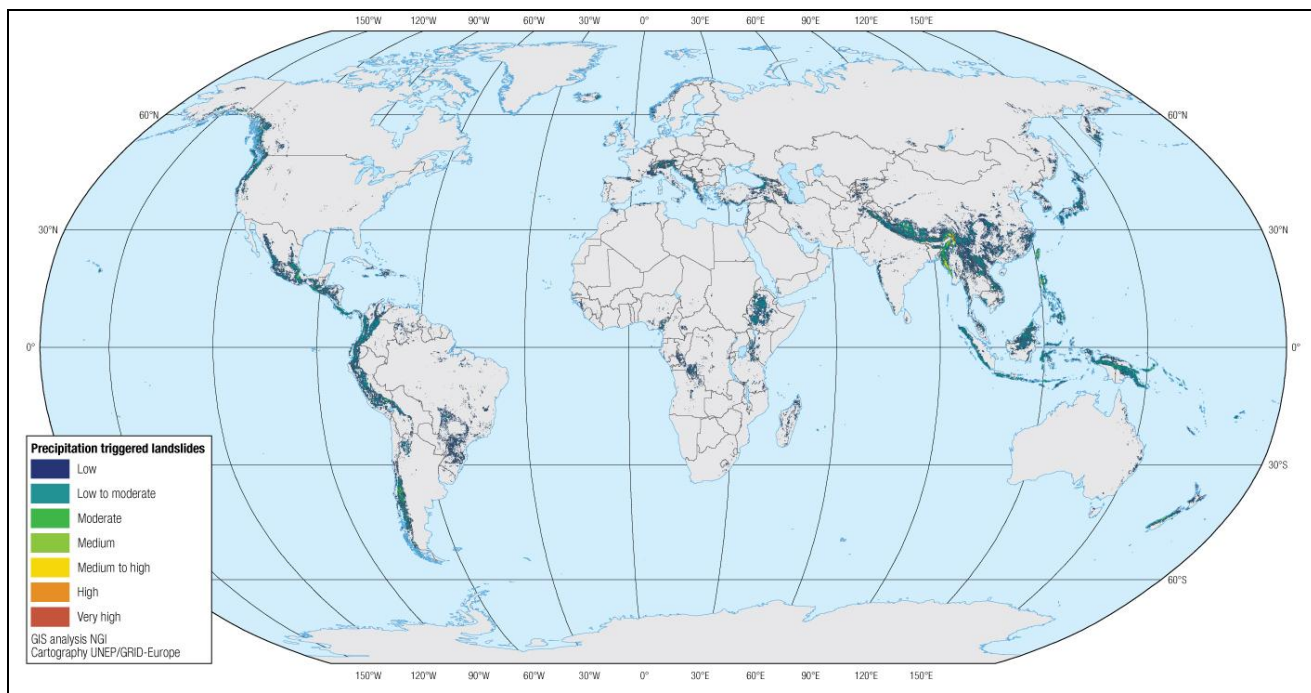


**Figure 14 Map of Earthquakes triggered Landslides Hazard distribution**

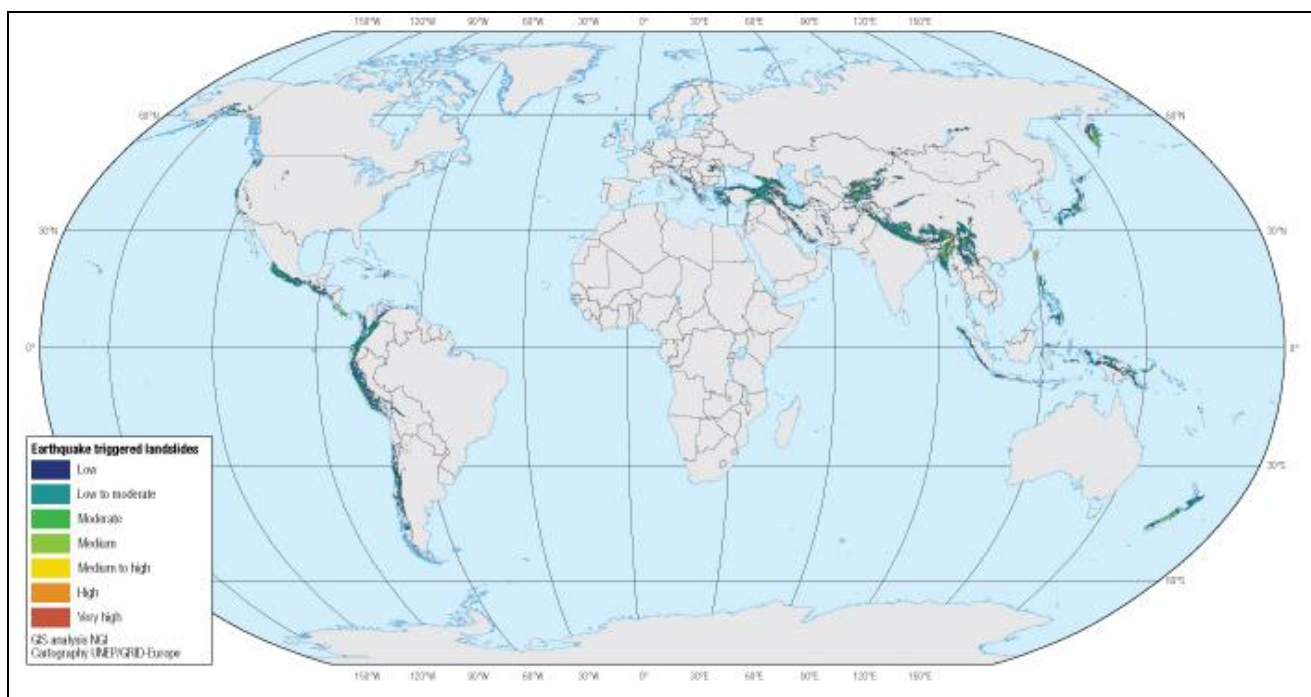
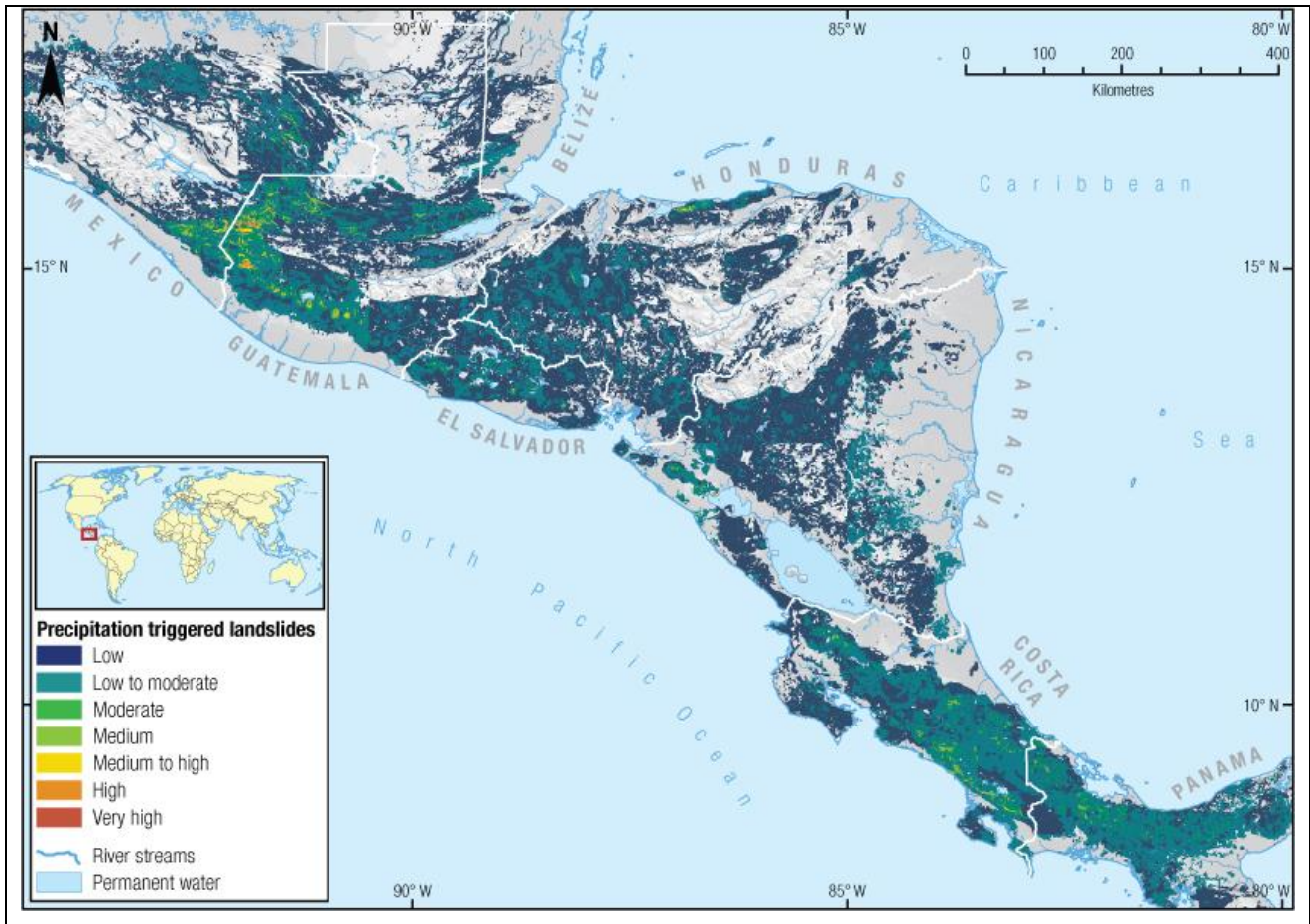


Figure 13 and

Figure 14 show the global distribution of Landslides around the world. The trigger influence is clearly visible by comparing both maps in areas like, Brasil, Africa, parts of Southeast Asia, etc.

**Figure 15 Zoom over central America for landslides triggered by precipitations**



### *Difficulties and limitations*

Human impact is a very important triggering factor for landslides, which is ignored in the model. On a global scale analysis, one could introduce an index that is related to population density and/or infrastructure density.

The lithology factor is probably the weakest link of the model, mainly because of the coarse resolution of the Geological Map of the World that has been used. We are not aware of any other similar database for global geology with a finer resolution. An index that could better describe the soil conditions would have made the model much better.

A universally accepted measure of landslide severity is not available at present. Some researchers define landslide intensity qualitatively as "a set of spatially distributed parameters describing the destructiveness of a landslide". In this context, landslide intensity has been addressed and defined quantitatively using a variety of parameters, such as maximum landslide velocity, total displacement, differential displacement (relative to points adjacent to the point under consideration), depth of the moving mass, depth of deposits after the movement ceases, depth of erosion, unit discharge, kinetic energy per unit area, maximum thrust, impact pressure, maximum normal or shear strain at or below ground surface, and so on.

In the present study, all landslides capable of causing injury or fatality are considered as "events". Beyond that, no attempt was made at considering the severity of different landslide events.

### *Next steps*

Some of the indices used in the present model for landslide hazard, for example the vegetation cover index or the lithology index, were only available at a crude resolution. It is expected that these data will be available at much better resolution in the coming years. Furthermore, several important factors that are known to influence the susceptibility to landslides, for instance the impact of human activities and effects of

deforestation, were not directly dealt with because of lack of data and/or availability of well-tested models. These factors could be included in future studies.

### **4.3. References**

#### *Articles and books*

- Lacasse, S. and Nadim, F. (2008). Landslide risk assessment and mitigation strategy. The First World Landslide Forum, United Nations University, Tokyo, Japan, 18-21 November.
- Mora, S. and Vahrson, W., 1994. Macrozonation methodology for landslide hazard determination, Bulletin of the Association of Engineering Geologists, Vol 31, No.1, 49-58.
- Nadim, F., Kjekstad, O., Peduzzi, P., Herold, C. and Jaedicke, C. (2006). Global landslide and avalanche hotspots. Landslides, Vol. 3, No. 2, 159-174.

### **4.4. Data Sources**

Elevation data (SRTM): Isciencs, Michigan, USA. <http://www.isciences.com/index.html>

Moisture index data: Climate Prediction Center, Maryland, USA.  
<http://iridl.ldeo.columbia.edu/SOURCES/.NOAA/.NCEP/.CPC/.GMSM/.w/>

Precipitation data: Global Precipitation Climatology Centre, Deutscher Wetterdienst, Offenbach, Germany.  
<http://gpcc.dwd.de>

Seismic trigger factor: Global Seismic Hazard Assessment Program (GSHAP), Geo Forschungs Zentrum, Potsdam, Germany. <http://seismo.ethz.ch/GSHAP/index.html>

Population data: Gridded Population of the World (GPWv3), Columbia University, New York, USA.  
<http://sedac.ciesin.columbia.edu/gpw/>

International disaster database: EM-DAT: The OFDA/CRED International Disaster Database, Université catholique de Louvain, Brussels, Belgium. <http://www.em-dat.net/>

Land cover database: Institute for Environment and Sustainability, Joint Research Centre, Ispra, Italy.  
<http://ies.jrc.ec.europa.eu/global-land-cover-2000>

## 5. Earthquakes

### 5.1. Authors

*Global Hazard distribution (UNEP/GRID-Europe)*

Bruno Chatenoux

*Case study on Sichuan (UNEP/GRID-Europe)*

A. De Bono

*Hazard methodology reviewed by:*

Avi Shapira (Israel Geophysical Institute, Israel)

Kunihiko Shimazaki (Professor, University of Tokyo, Japan)

Giuliano Panza (Professor, University of Trieste, Italy ICTP)

Mihail Garevski (Director, Institute of Earthquake Engineering and Engineering Seismology, Former Yugoslav Republic of Macedonia)

### 5.2. Hazard

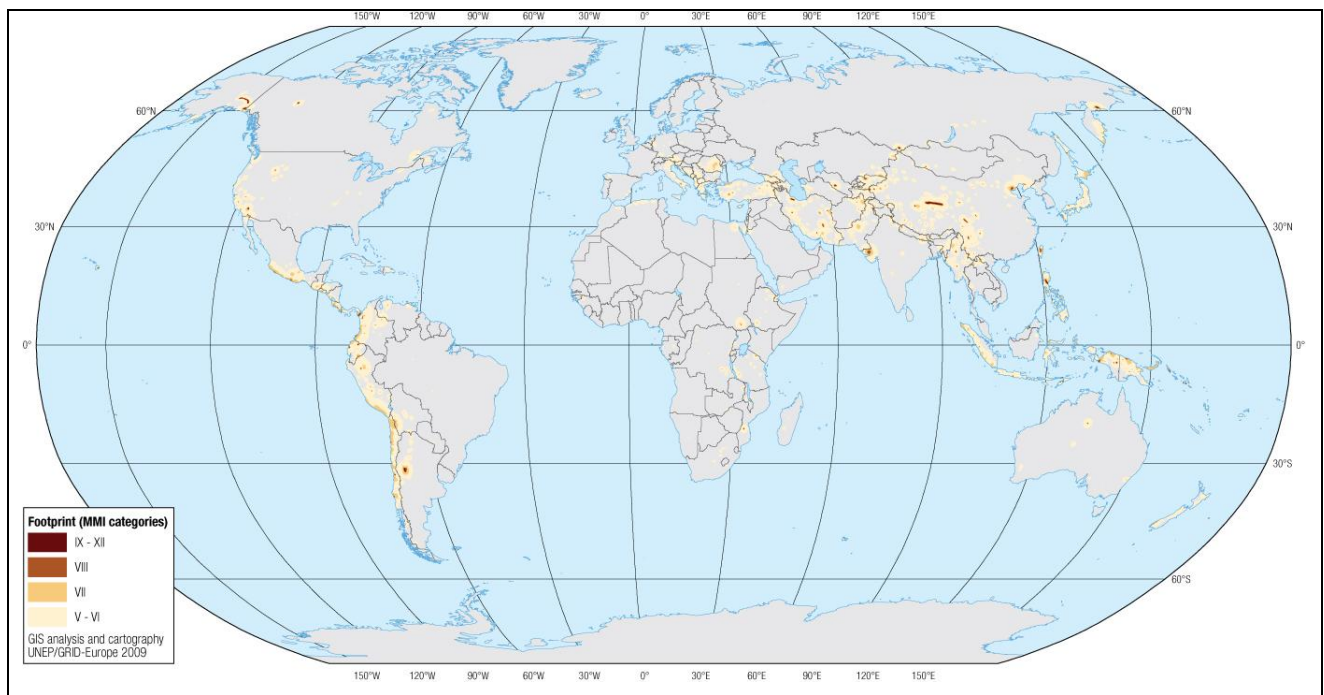
The term earthquake is used to describe any seismic event that generates seismic waves. They are caused mostly by rupture of geological faults and sometimes also by volcanic activity, landslides, etc, and are concentrated within specific areas around the world, mainly in geologically active areas such as the Pacific coast on North and South America, Indonesia, Japan, Himalayas, etc (see Figure 16).

Two methods were explored for earthquakes. The first one, developed by Arthur Lerner-Lam and Liana Razafindrazay from Columbia University (New York, USA) for producing the map of hazard distribution. The researchers from Columbia University use the estimate of ground motion exceedance probabilities derived from seismicity catalogs has been produced by the Global Seismic Hazard Assessment Program (GSHAP). The original GSHAP estimations of ground acceleration exceedance probabilities was used, calculated as a 10% chance in 50 years. This equates to a return period of 500 years for a specific level of ground acceleration at a specific location.

While ground acceleration exceedance probabilities are useful for engineering calculations, it is necessary to calibrate ground accelerations against recorded damage and casualties in the absence of first order information of physical earthquake vulnerabilities. To do so, probabilistic ground acceleration has been converted to probabilistic Modified Mercalli Intensity (MMI) using empirical conversion factors determined by Wald et al. (1999), using a formulation developed by Trifunac and Brady (1975). This model was produced by University of Columbia and was used for the hazard distribution.

Although useful for mapping potential distribution of earthquakes hazard intensity, an alternative method was applied for computing exposure to earthquakes. The reason being that non-exceedance probability do not provide information on more frequent, alas less intense earthquakes at a specific location. To overcome this issue, the exposure was based on past earthquakes intensity as modelled by the United States Geological Survey and further refined by UNEP/GRID-Europe as explained below.

**Figure 16 Global earthquake hazard**



Even if an earthquake is located in a given location it generates a range of peak ground shaking levels at sites throughout the region.

The best actual dataset of ground shaking triggered by earthquakes has been created and is distributed by the USGS / Earthquake Hazards Program under the name of Shakemap Atlas V.1.

The Atlas provides maps for approximately 5,000 recent and historical global earthquakes. Maps are available for several parameters: peak horizontal acceleration (PGA, cm/s<sup>2</sup>), peak horizontal velocity (PGV, cm/s), spectral response for three periods of time (0.3, 1.0 and 3.0 seconds) and instrumental intensity (MMI) (Wald and others 1999, 2005; Wald and Allen 2007). This is the last category that has been used in the present study as it makes it easier to relate the recorded ground motions to the expected felt and damage distribution.

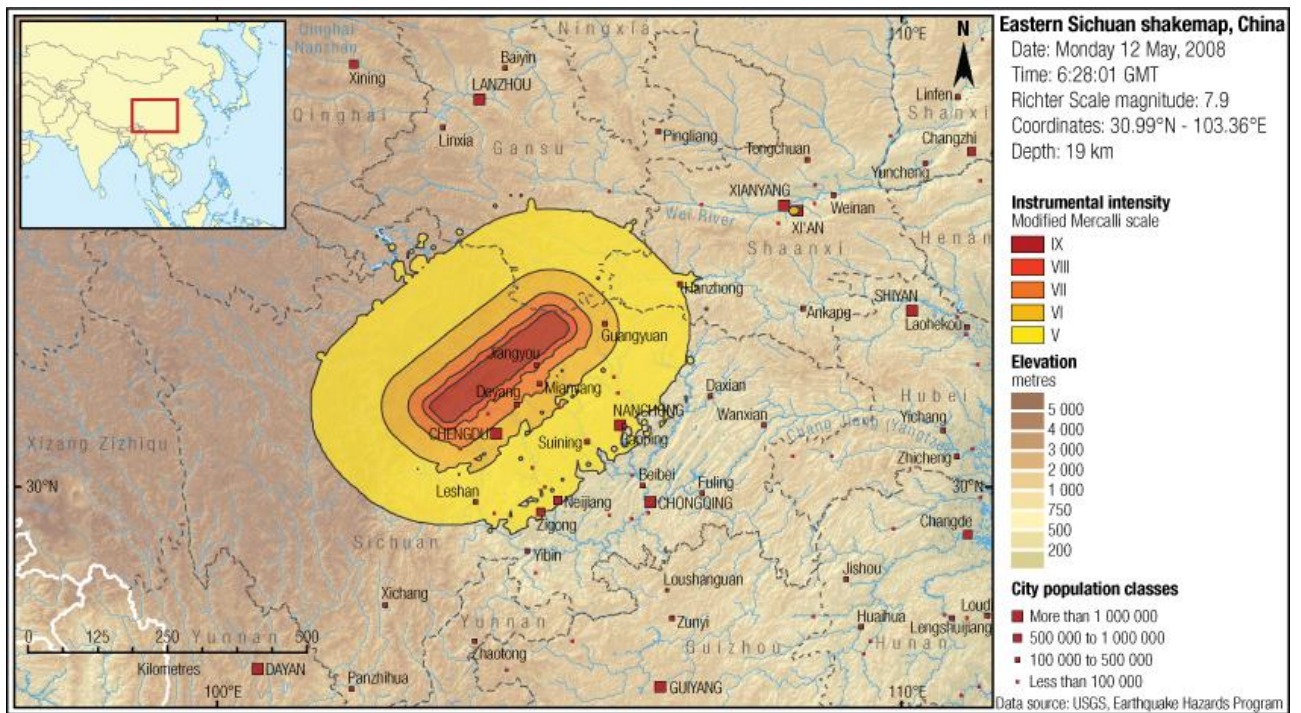
**Modelling Modified Mercalli Intensities (MMI)**

Simulated intensities are based on a combination of peak acceleration and velocity amplitudes regression. They depend on multiple parameters that are:

- distance from the earthquake,
- complexities in the structure (fault rupture specificities) and type of earth crust,
- local rock and soil condition, site amplification approximated from topographic gradient and share-wave velocity.

Simulated values are finally corrected in function of observed values (see Figure 17).

**Figure 17 MMI shakemap for Eastern Sichuan 2008 earthquake, China**



The MMI intensity scale classifies the severity of earthquake shaking on a scale of I to XII. The lowest intensities are not felt by people, while the highest intensities correspond to nearly total destruction of all constructed facilities. The MMI categories were finally classified into 4 earthquake hazard categories for this study: negligible, low, moderate, and high (see Table 3).

**Table 3 Modified Mercalli Index and earthquake hazard categories used within the project**

Perceiving shake	Not felt	Weak	Light	Moderate	Strong	Very strong	Severe	Violent	Extreme
Potential damage	none			Very light	Light	Moderate	Moderate/Heavy	Heavy	Very heavy
MMI	I	II-III	IV	V	VI	VII	VIII	IX	X+

<b>Hazard category</b>				<b>negligible</b>	<b>low</b>	<b>moderate</b>	<b>high</b>
------------------------	--	--	--	-------------------	------------	-----------------	-------------

*From MMI to frequencies*

Finally annual frequency grids have been processed for MMI categories by summing the number of times each pixel has been affected by a given category and dividing the total by the length of the dataset period.

*Difficulties and limitations*

Shakemaps representativeness varies greatly around the world due to the wide variation in the availability, resolution and completeness of the necessary data input, as well as the presence of measuring stations. Due to these reasons proper local algorithms are missing and local ones have been extrapolated globally.

*Next steps*

Completion and improvement of the resolution of the needed data input, as well as the setting up of new monitoring stations are the necessary prerequisite in order to refine the wave propagation algorithms, improve the models and consolidate their validation

**5.3. References**

Allen, T. I., D. J. Wald, Hotovec, A, Lin, K, Earle, P., and K. Marano (2008). "An Atlas of ShakeMaps for Selected Global Earthquakes." U.S. Geological Survey Open File Report 2008-1236, 47 pp.

Wald, D.J., and Allen, T.I., 2007, Topographic slope as a proxy for seismic site conditions and amplification: Bull. Seism. Soc. Am., v. 97, no. 5, p. 1379-1395.

Wald, D.J., Quitoriano, V., Heaton, T.H., Kanamori, H., Scrivner, C.W., and Worden, B.C., 1999, TriNet "ShakeMaps": Rapid generation of peak ground-motion and intensity maps for earthquakes in southern California: Earthquake Spectra, v. 15, no. 3, p. 537-556.

Wald, D.J., Worden, B.C., Quitoriano, V., and Pankow, K.L., 2005, ShakeMap manual: technical manual, user's guide, and software guide: U.S. Geological Survey, 132 p.

**5.4. Data sources**

Shakemap Atlas: <http://earthquake.usgs.gov/eqcenter/shakemap/atlas.php>

## 6. Tsunamis

### 6.1. Authors

*Hazard model* (International Centre for Geohazards / NGI)

F. Løvholt  
N. Zamora  
S. Glimsdal  
G. Yetman  
H. Smebye

*Hazard methodology reviewed by:*

Jörn Behrens (PD. Dr., Alfred Wegener Institute for Polar and Marine Research, Germany)  
Stefano Tinti (Professor, University of Bologna, Italy)  
Kenji Satake (Professor, University of Tokyo, Japan)

### 6.2. Hazard

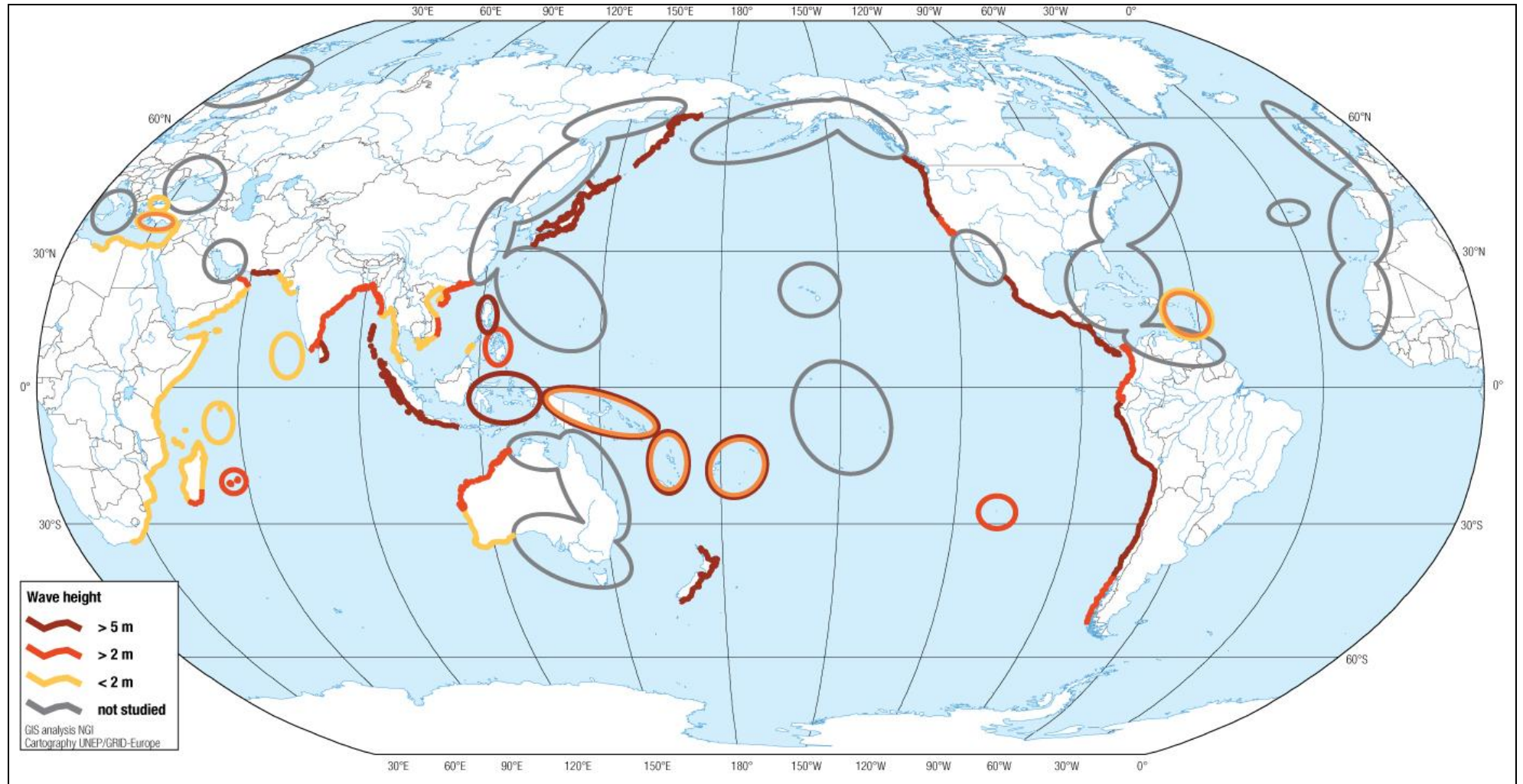
Tsunamis are waves set in motion by large and sudden forced displacements of the sea water, having characteristics intermediate between tides and swell waves. Although tsunamis are infrequent (ca. 5-10 events reported globally pr. year), they do represent a serious threat to the coastal population in many areas, as demonstrated by the devastating effects of the 2004 Indian Ocean tsunami. Tsunamis are often generated by submarine earthquakes. However, submarine landslides are becoming increasingly recognized as important triggers as well. Other sources of tsunamis include collapsing/exploding volcanoes, and asteroid impacts. Tsunamis generated by large earthquakes in subduction zones (area where one continental plate moves beneath another) along the major plate boundaries contribute most to the global tsunami hazard.

When the tsunami is generated, it propagates in the open sea with speeds of several hundred kilometres per hour, and may hence reach coastlines distant from the earthquake within a relatively short time. The wave slows down when it reaches the shoreline, and its height increases. Because of its relatively large wave-length, the tsunami may travel far inland compared to wind waves and swells, and because of its relatively short period, it inundates much faster than tidal waves and storm surges. When the tsunami inundates land, flow velocities become large, enabling the tsunami to carry very large objects, erode the landscape, and destroy buildings. The tsunami becomes lethal both due to possibilities of being impacted by debris and flotsam, as well as drowning. Generally, tsunamis may cause damage to most coastal structures; however, buildings of poor quality are particularly vulnerable. The tsunami is most destructive close to the shoreline where the flow velocity and wave load are largest.

The results of the present study represent a first-pass assessment of the tsunami hazard and population exposure based on today's knowledge. The study considered the tsunamis caused by earthquakes only, as these events will often contribute more to the risk than the smaller events. Tsunamis caused by landslides, rockslides, and volcanoes were not included in this study. Some countries potentially affected by tsunamis are not included in this study, examples are Italy, Morocco, Korea, some parts of USA, Russia, China.

Tsunami hazard is a combination of anticipated wave-height, travel time and exposed population within a region.

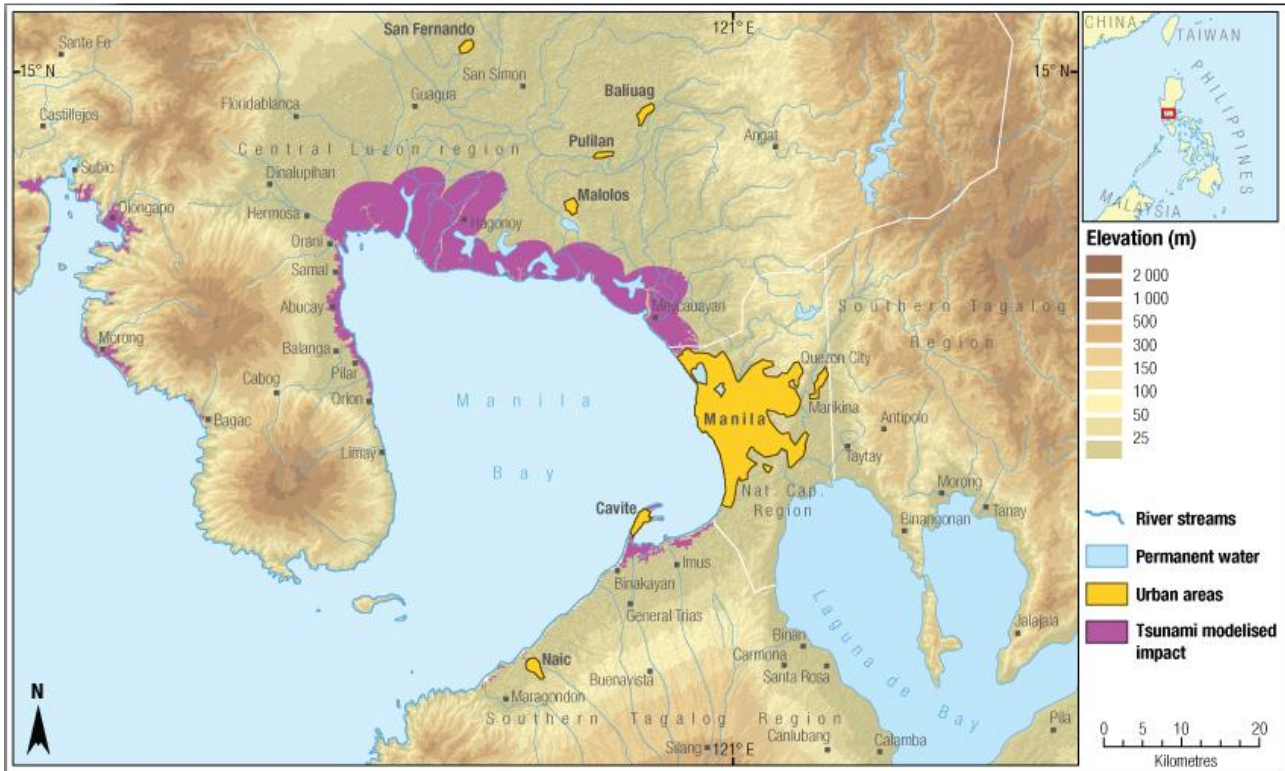
Figure 18 Rough sketch of the global tsunami hazard in terms of tsunami wave-height ( $\square$ ) and travel time (t). Some important areas omitted in this study are also sketched.



### Modelling tsunami

The objective of this study is to make optimal use of completed and ongoing studies of tsunami hazard. A comprehensive list of reports and scientific papers have been compiled and utilised in producing tsunami hazard maps (Figure 18) as well as finding return periods of future events. Additional hazard maps have been produced by applying numerical tsunami models and zooming over a selected area (Figure 19).

**Figure 19 Tsunami modelling in the Manila bay (Philippines)**



Large and highly destructive tsunami events like the 2004 Indian Ocean tsunami, generally pose greater risk to human lives than smaller and more frequent events. For this pilot study, the development of the tsunami hazard maps focuses on extreme events only, that is, tsunamis generated by large earthquakes having return periods of approximately 500 years (formally, a probability of 10 % of an event occurring in 50 years). The probabilities of such infrequent events are generally hard to establish due to the lack of a reliable long-term history in monitoring the earthquakes generating the tsunamis as well as the tsunamis themselves. In establishing the return periods, the study has relied heavily on a patchwork of different methods and information obtained from literature, including ancient records of tsunamis and earthquakes, seismological records, or derived from the probability from the motion of the continental plates.

### Intensity

Several tsunami intensity scales exist today, and most of them are functions of the maximum run-up on land of the tsunami. In our study intensity measure is combining information of the maximum run-up with the destruction is the revised Ambraseys-Sieberg intensity scale (see the Tsunami Glossary at International Tsunami Information Centre; <http://ioc3.unesco.org/itic/>). The shoreline wave-height is actually used as the measure of the tsunami severity.

Another parameter not directly linked to the tsunami intensity but that has a strong influence on the early warning system is the time needed by the tsunami to reach the coastline. Table 4 lists the top 12 countries that would potentially be hit by a tsunami in less than 15 minutes.

**Table 4 Minimum tsunami arrival delay –Top 12 with less than 15 minutes**

Country	Elev_max
Chile	22.39
Greece	2.9
India	7.7

Indonesia	15
Myanmar	6
Peru	22.63
Salomon Islands	10
Portugal	37.1
Tonga	6.1
Pakistan	14.3
Papua New Guinea	19.1
Philippines	15.6

#### *Difficulties and limitations*

For this pilot study, the tsunami hazard maps are focussing on extreme events only, that is, tsunamis generated by large earthquakes of return periods of approximately 500 years. It is noted that establishing the size of such infrequent tsunamis are uncertain due to the lack of a reliable long term history in monitoring the earthquakes generating them. Hence, the return periods for the future tsunamis are not to be interpreted as precise estimates. Another assumption in this study is also that the earthquake generation is so called “memory free”, meaning that the probability of a future event is independent of the occurrence recent events.

Due to the challenging task of covering the whole world, emphasis is given to producing regional hazard maps for less developed countries rather than for countries clearly able to cope with tsunami risk themselves. The methods for establishing the global tsunami hazard maps and population exposure are established based on approximate and simplified methods for covering large geographical areas. Some countries potentially affected by tsunamis are not included in this study, examples are Italy and Portugal. Tsunamis generated by landslides, rockslides, and volcanoes are also not included in this study.

#### *Next steps*

To complete this study, the tsunami hazard and exposed population should be established for other return periods than 500 years. Future studies should also take into account information on recent earthquake events by utilising the so called GAP analysis, which will include a possibility of distributing the tsunami generation potential more locally. Means to include the tsunami vulnerability with main priority to the tsunami mortality are key elements that must be performed to enable comparison with other hazards. The current study do not include tsunami risk from non-seismic sources, these should be included in future revisions. Other improvements that should be performed include updated methods for computing the tsunami inundation, more dense samples of results, as well as studying hotspot areas currently not included in the present study.

### **6.3. References**

#### *Articles and books*

Annaka, T., K. Satake, T. Sakakiyama, K. Yanagisawa and N. Shuto (2007): Logic-tree approach for probabilistic tsunami hazard analysis and its applications to the Japanese coasts. *Pure and Applied Geophysics* 164, pp 577–592.

Burbidge, D., Cummins, P., and Mlezcko, R., (2007): A Probabilistic Tsunami Hazard Assessment for Western Australia. Report to the Fire and Emergency Services Authority of Western Australia.

Gonzalez, F. et al. (2006): Seaside, Oregon Tsunami Pilot Study—Modernization of FEMA Flood Hazard Maps. Joint NOAA/USGS/FEMA Special Report.

GNS (2005): Review of Tsunami Hazard and Risk in New Zealand. Institute of Geological & Nuclear Sciences client report 2005/104

NGI (2006) - Tsunami Risk Reduction Measures with Focus on Land use and Rehabilitation, technical report. Available at (<http://www.ngi.no/en/Contentboxes-and-structures/Reference-Projects/Reference-projects/The-Risk-of-Tsunamis-in-Southeast-Asia/>)

#### *Internet references*

International Oceanic Commission (<http://www.ioc-tsunami.org/>)

#### 6.4. Data sources

Region	Method	Reported metric	Reference
Indonesia - Banda Ache	Credible worst case	Run-up	Sengara et al. (2008)
Western Thailand	Credible worst case	Shoreline surface elevation	Løvholt et al. (2006)
Western Australia and southern Java	Probabilistic	Surface elevation at 50m water depth	Burbidge et al. (2007)
Indonesia - Makassar Strait	Probabilistic	Run-up	Prasetya et al. (2001)
South China and Taiwan	Probabilistic	Run-up	Liu et al. (2007)
Japan – East coast	Probabilistic	Run-up	Annaka et al. (2007)
Japan – West coast	Historical records	Run-up	Rikitake and Aida (1998) - from Shimazaki (1984)
Russia - Kamchatka	Historical records	Run-up	Kaistrenko et al. (2003)
New Zealand	Probabilistic	Run-up	Berryman et al. (2006)
USA - Puerto-Rico	Probabilistic	Run-up	Mercado (2001)
El Salvador	Probabilistic	Run-up	Brizuela (2005)
Mexico	Probabilistic	Run-up	Geist and Parsons (2006)
USA - Southern California	Probabilistic	Run-up	Legg et al. (2004)
USA – Oregon	Probabilistic	Run-up	Gonzales et al. (2006)
USA - Washington state	Credible worst case	Run-up	Venturato et al. (2007)
USA - Washington state	Credible worst case	Run-up	Venturato et al. (2004)
Canada - Vancouver Island	Historical records	Run-up	Clague et al. (2000)
Eastern Mediterranean	Credible worst case	Run-up	Salamon et al. (2007)
Greece - Gulf of Corinth	Probabilistic	Run-up	Tselentis et al. (2006)
Turkey - Sea of Marmara	Credible worst case	Run-up	Hebert et al. (2005)
Spain - Balearic Islands	Credible worst case	Run-up	Roger and Hebert (2008)

**Table 5 Literature sources for tsunami hazard maps**

## 7. Biomass fires

### 7.1. Authors

*High temperature event detection (ESA)*

O. Arino

S. Plummer

S. Casadio

*Global biomass fires distribution (UNEP/GRID-Europe)*

P. Peduzzi

### 7.2. Hazard

According to a recent inventory (Tansey et al. 2008), wild land fires and other biomass fires annually burn a total land area of between 3.5 and 4.5 million km<sup>2</sup>, equivalent to the surface area of India and Pakistan together, or more than half of Australia. This makes it one of the most spatially prevalent hazards after drought.

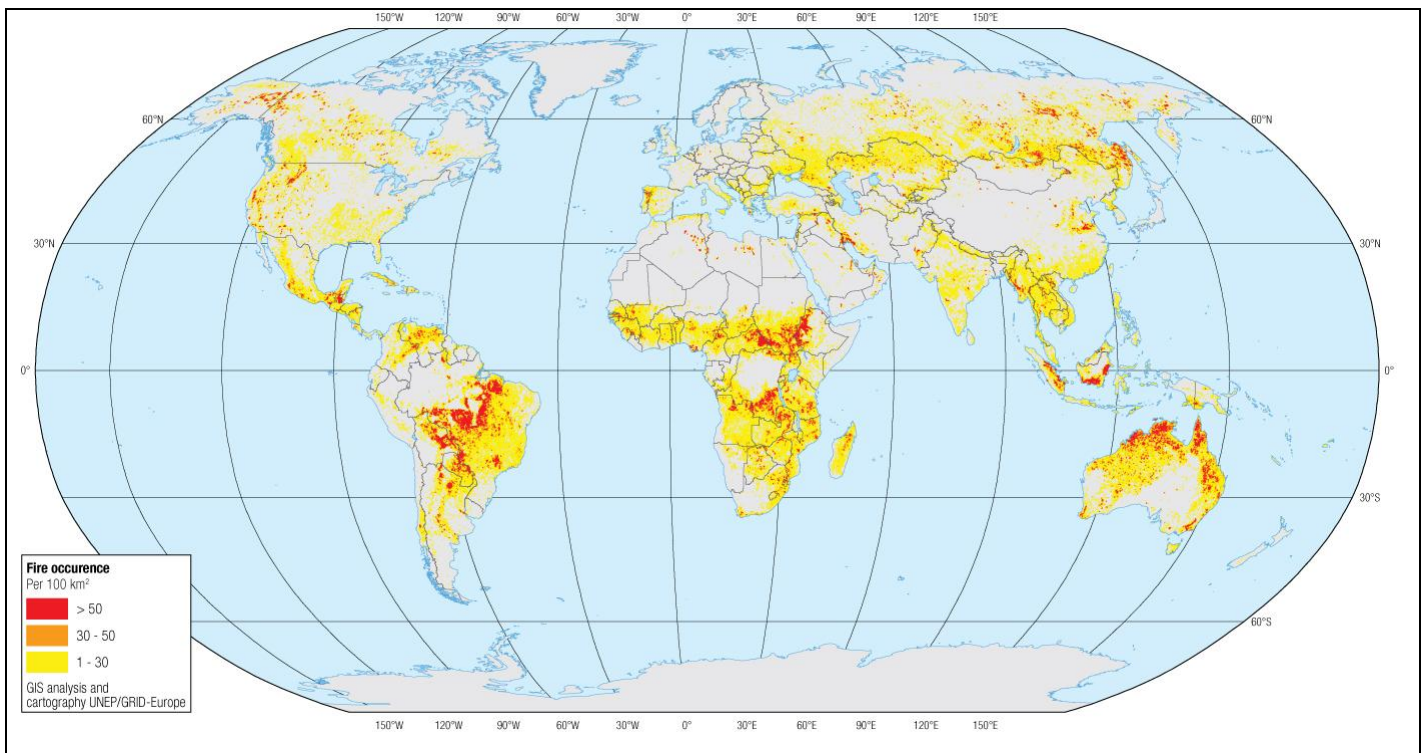
Emissions from biomass burning inject pollutants into the atmosphere, as well as greenhouse gases (GHG). The IPCC attributes 17.3% of total anthropogenic emissions to biomass burning, making it the second largest source of GHG from human activities after the burning of fossil fuel. However, this figure may in reality be even higher, as it is based on pre-2000 data. Biomass fire is the only hazard that has both an impact on, and is exacerbated by, climate change. Most fires have human causes.

#### *Modelling Fires*

The algorithm 1 product of WFA dataset (that records at night each 1x1 km pixel that exceed a temperature value of 312 °K, with an average revisiting period of 3 days) has been downloaded on a monthly basis and merged as one single point geodataset containing more than a million events for the period (1997 – 2008).

A yearly average density grid has been processed by counting the fires located within each 0.1 decimal degree pixel divided by the length of the time period (see Figure 20). Not all high temperature events are biomass fires, as gas flares and other high temperature events are also detected. However, most fires are due to biomass burning.

**Figure 20 Average yearly density of fires**



### **7.3. References**

#### *Articles and books*

Arino, O., Plummer, S. and Casadio, S. (2007), Fire Disturbance: the Twelve years time series of the ATSR World Fire Atlas. Proceedings of the ENVISAT Symposium 2007, SP-636, ESA

IPCC (2007). Climate change 2007: Synthesis Report, p.36. [http://www.ipcc.ch/pdf/assessment-report/ar4/syr/ar4\\_syr.pdf](http://www.ipcc.ch/pdf/assessment-report/ar4/syr/ar4_syr.pdf)

Lehsten, V., Tansey, K., Balzter, H., Thonicke, K., Spessa, A., Weber, U., Smith, B., and Arneeth, A.(2009). Estimating carbon emissions from African wildfires. Biogeosciences, 6, 349-360.

### **7.4. Data sources**

#### *High temperature events detection*

European Space Agency (ESA-ESRIN), World Fires Atlas Program (ATSR) <http://dup.esrin.esa.it/ionia/wfa/index.asp>, From January 1997 to December 2008, Algorithm 1

## 1.2 Extraction of exposure and others parameters

In order to be able to calculate exposure, analyse and finally simulate the risk induced by each hazard, the extraction of several parameters has been necessary.

However as the geodata format was different in function of the type of hazard, the extraction of exposure and others parameters use to vary. Yet three main processes have been applied and are synthesised in the Table 6 and are developed in the three following chapters.

**Table 6 Extraction process in function of geodata format**

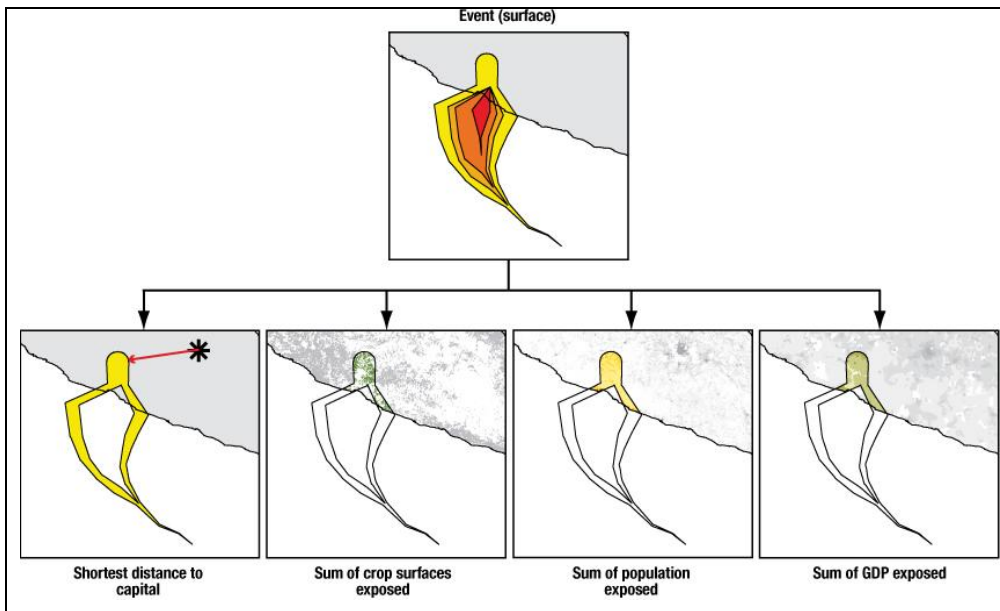
	Event per event	Frequencies	% of pixel
Cyclones	x		
Surges	x		x
Earthquakes	x		
Floods		x	
Droughts		x	
Landslides		x	
Tsunamis		x	

### *Event per event processing*

The extraction has been done for each non overlapping category of each event. In the case one event affected more than one country affected areas have been split for each country. Each part being treated as a single event, and the following information extracted (see Figure 21) for a given reference year:

- Shortest distance to capital in kilometres,
- Sum of crops surfaces exposed in km<sup>2</sup>,
- Sum of population exposed (inhabitants),
- Sum of GDP exposed in US \$.

**Figure 21 Geoprocessing flow, in this case Saffir-Simpson category 1 of Madeline cyclone that hit Mexico in 1976**



The distinction between urban and rural region has also been taken into account during the extraction of the population and the GDP affected. Additionally the period of the day (day or night) has also been included into account in the earthquakes analysis.

The Figure 22 and Table 7 illustrate how a single event (in this case the 22<sup>nd</sup> November 1995 earthquake in Red Sea region) has been split into 10 different parts (4 in Egypt, 1 in Israel, 1 in Jordanian and 4 in Saudi Arabia).

**Figure 22 Earthquake that affected several countries in the red Sea region**

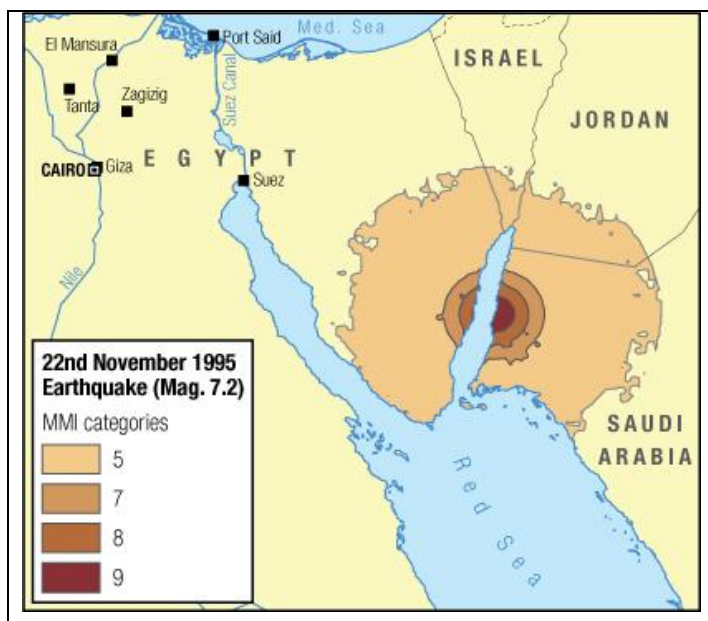


**Table 7 Values 2007 for the example in Figure 22**

Country	MMI	Urban population 2007	Rural population 2007	Total population 2007	Urban GDP 2007	Rural GDP 2007	Total GDP 2007	Crops area	Distance to capital
EGY	5	9	62,335	62,344	23,080,972	47,575,624	70,656,596	0	228
EGY	7	0	1,168	1,168	0	3,006,869	3,006,869	0	327
EGY	8	0	2,495	2,495	0	3,430,351	3,430,351	0	338
EGY	9	0	0	0	0	6,454	6,454	0	352
ISR	5	50,619	5,659	56,278	309,884,064	43,787,116	353,671,180	0	193
JOR	5	124,909	10,031	134,940	248,821,568	15,625,906	264,447,474	0	219
SAU	5	1,874	26,032	27,906	344,615,712	244,939,807	589,555,519	2	0
SAU	7	0	1,521	1,521	0	23,650,802	23,650,802	0	1,224
SAU	8	0	11	11	0	14,164,395	14,164,395	0	1,241
SAU	9	0	4	4	0	9,325,915	9,325,915	0	1,254

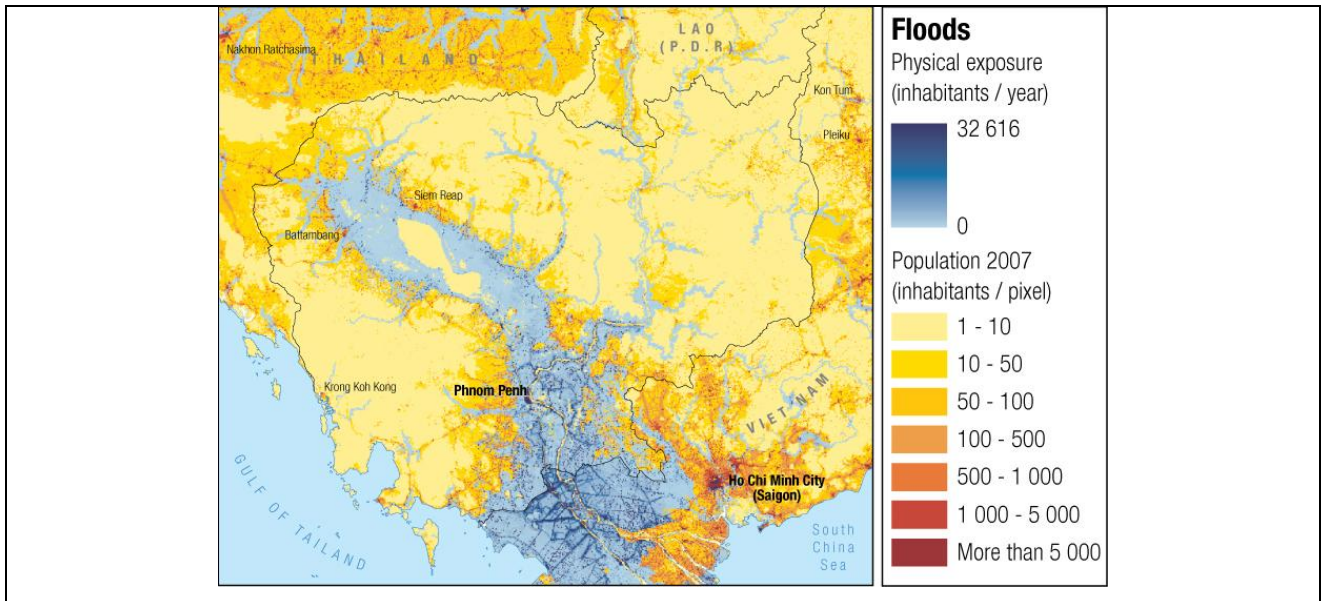
The same information has been extracted for the reference years 1975, 1990 and the event's year in order to define time trend lines.

### ***Frequencies processing***

When the event per event information was not available, the exposition has been extracted from frequency grids at country level applying the following procedure:

- Pixel exposition calculated by multiplying the frequency grid (average number of event per year) by the parameter to be extracted grid (population, GDP or crops surfaces) see Cambodia example in Figure 23,
- Summing the exposition grid by country extent gave the total country exposition to the parameter.

**Figure 23 Cambodia region population in orange, population exposed to floods in blue**

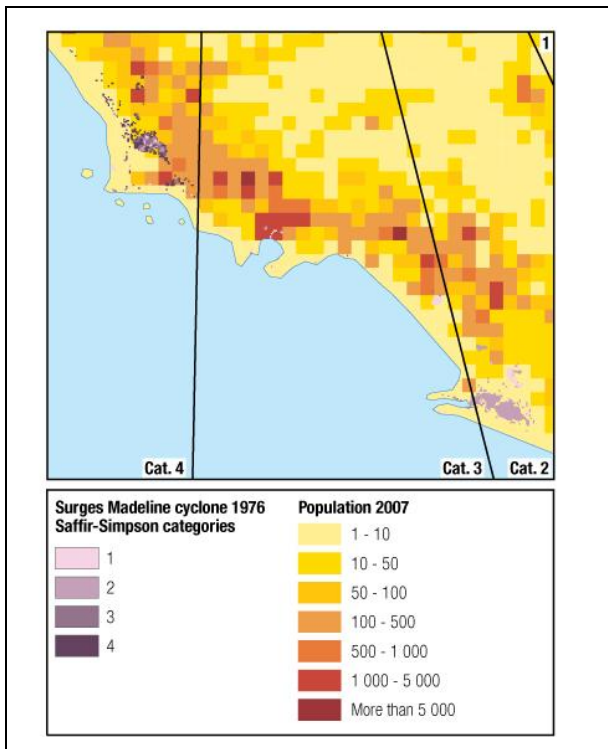


Once again, an urban/rural mask has been applied, obtaining the population exposure, economical exposure for a given year, as well as the crop exposure. Minimum distance to capital has been impossible to calculate as it is based on an event per event information.

**Percentage of pixel affected processing**

A particular process has been developed specifically for the surge hazard simulated at high resolution (90 meter resolution of the Digital Elevation Model<sup>3</sup>, see the tiny blue pixels in Figure 24).

**Figure 24 Zoom on Madeline cyclone inundated areas**



<sup>3</sup> [www2.jpl.nasa.gov/srtm/](http://www2.jpl.nasa.gov/srtm/)

In this case a percentage of each pixel affected by a given hazard over a given period has been calculated, representing the intensity of the hazard on the area. This percentage has then be applied during the exposition calculation. In other word, only the percentage of the parameter (population, GDP or crops surfaces) corresponding to the percentage of pixel exposed has been taken into account.

**Table 8 Values 2007 for the example in Figure 24**

ISO3	Saffir-Simpson category	Crop area	Urban population 2007	Rural population 2007	Total population 2007	Total population 2007
MEX	1	0	0	1,864	1,864	9,759,215
MEX	2	0	0	439	439	2,091,688
MEX	3	0	0	218	218	3,382,470
MEX	4	0	0	471	471	5,975,114

### **Data sources**

#### *Population*

Two sources have been used for the population extraction. Yearly grids have been generated by CIESIN, Columbia University from the Global Rural Urban Mapping Project (GRUMP). GRID-Europe performed the same task using the LandScan data set from LandScan™ Global Population Database. Oak Ridge, TN: Oak Ridge National Laboratory<sup>4</sup>.

#### *GDP*

The World Bank prepared and provided access to the yearly GDP data set.

#### *Urban/Rural*

An Urban/Rural mask has been prepared by GRID-Europe on the base of ESA/JRC GlobCover 2005.

#### *Crops*

The global crops dataset is issued from the Global Land Cover 2000 (GLC2000) crops area (class 16)

#### *Capitals*

For Data sources on hazard, please check in the related hazard annexe.

---

<sup>4</sup> [www.ornl.gov/landscan/](http://www.ornl.gov/landscan/)